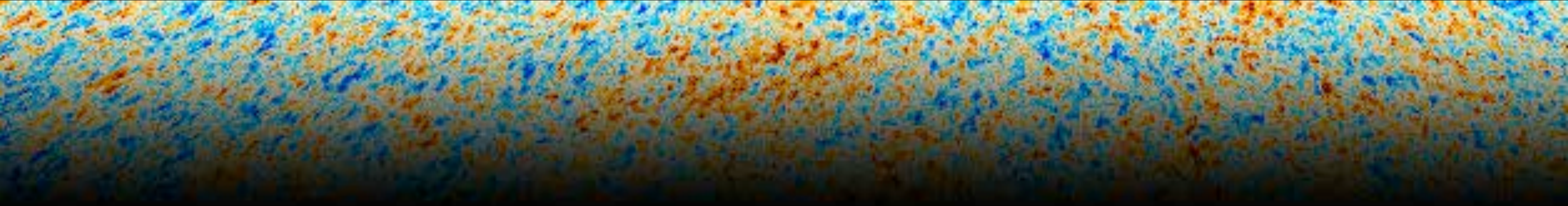

Review of Hubble Measurements

Raphael Flauger

LHC Results Forum & KITP, February, 28 2020

The Hubble tension

CNN **World** Africa Americas Asia Australia China Europe India Middle East United Kingdom

(CNN) — The universe is expanding 9% faster than scientists expected, according to a new study. And new physics may be required to understand why.

Although scientists have suggested for years that this faster expansion rate was true, new measurements collected by NASA's Hubble Space Telescope helped make the confirmation.

The expansion rate is at odds with the universe's trajectory shortly after the Big Bang, more than 13 billion years ago. That trajectory was measured by the European Space Agency's Planck satellite. The satellite was able to map an afterglow from 380,000 years after the Big Bang, called the Cosmic Microwave Background, allowing for a prediction of the universe's evolution.

The Hubble tension

"The Hubble tension between the early and late universe may be the most exciting development in cosmology in decades," said Adam Riess, study author, distinguished professor of physics and astronomy at the Johns Hopkins University and Nobel laureate. "This mismatch has been growing and has now reached a point that is really impossible to dismiss as a fluke. This disparity could not plausibly occur just by chance."

Riess is leading a project called the SH0ES team that worked on this research.

Planck

ESA satellite mission that observed the microwave sky from 2009 until 2013

(Planck 2018 IV)

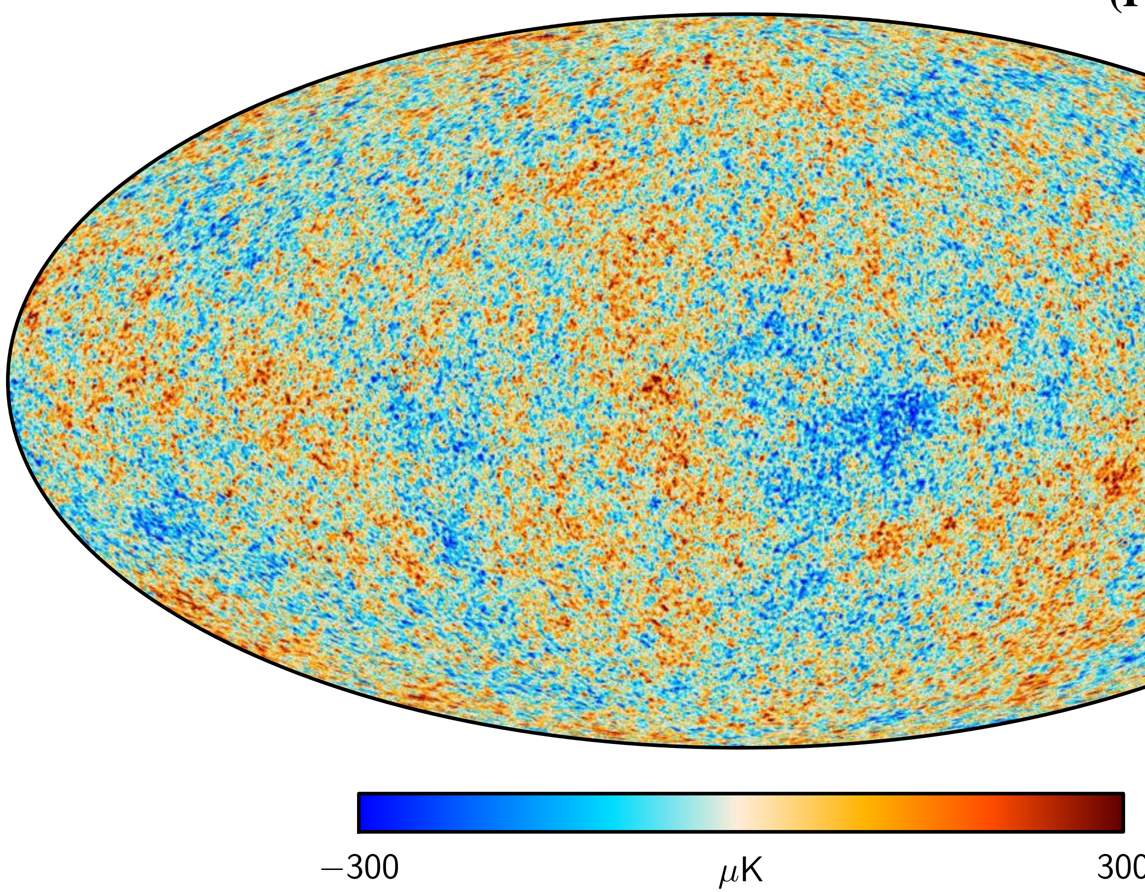

Planck

Angular power spectrum of CMB temperature anisotropies

(Planck 2018 VI)

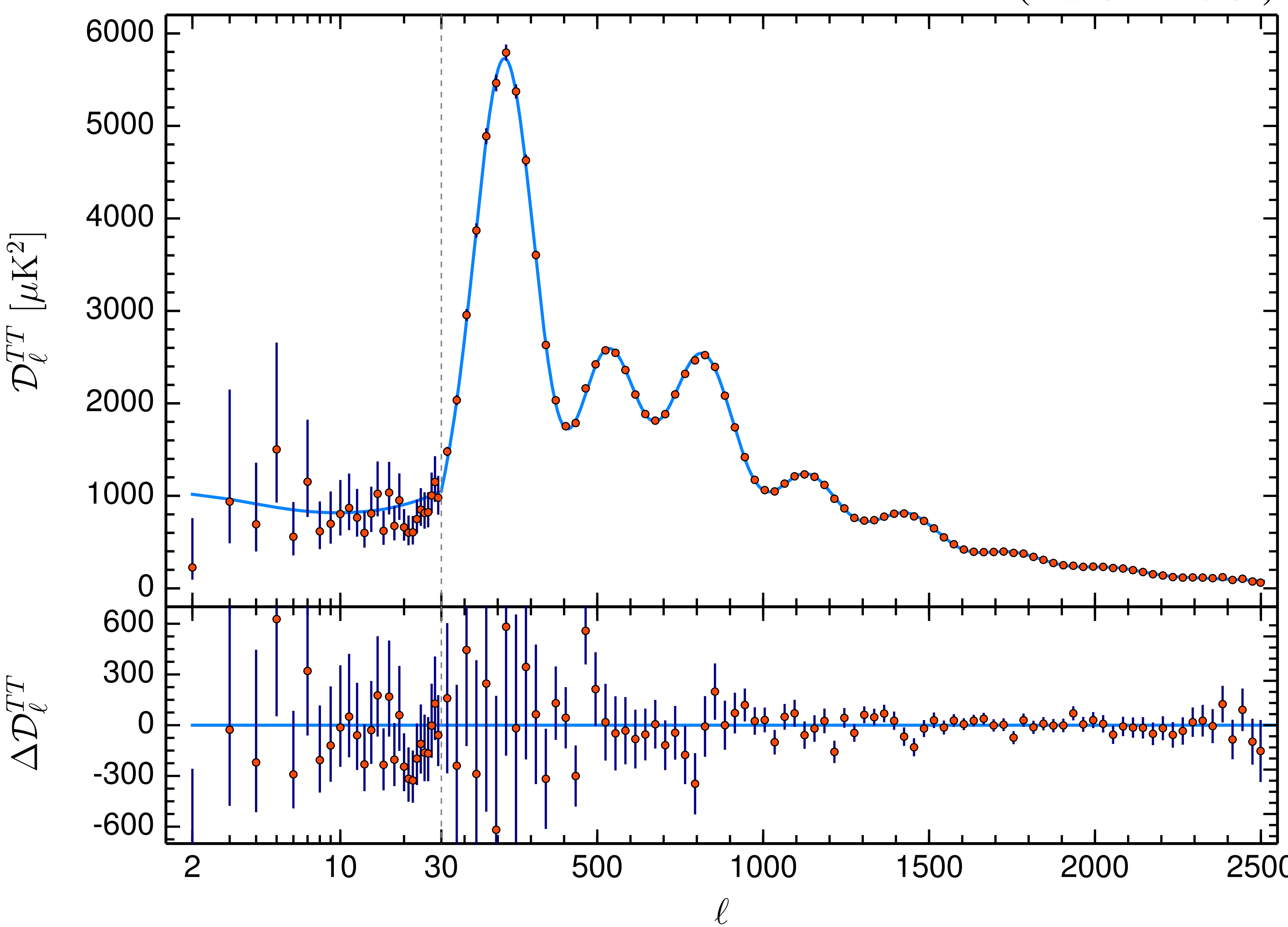

Planck

The early universe is remarkably simple and the CMB data is in good agreement with the six-parameter LCDM model.

Parameter	TT,TE,EE+lowE+lensing 68% limits
$\Omega_b h^2$	0.02237 ± 0.00015
$\Omega_c h^2$	0.1200 ± 0.0012
$100\theta_{MC}$	1.04092 ± 0.00031
τ	0.0544 ± 0.0073
$\ln(10^{10} A_s)$	3.044 ± 0.014
n_s	0.9649 ± 0.0042
H_0 [km s^{-1} Mpc^{-1}] . .	67.36 ± 0.54
Ω_Λ	0.6847 ± 0.0073
Ω_m	0.3153 ± 0.0073

* the sum of the neutrino masses is kept fixed at 0.06 eV

SH$_0$ES

Supernovae, H_0, for the Equation of State of dark energy

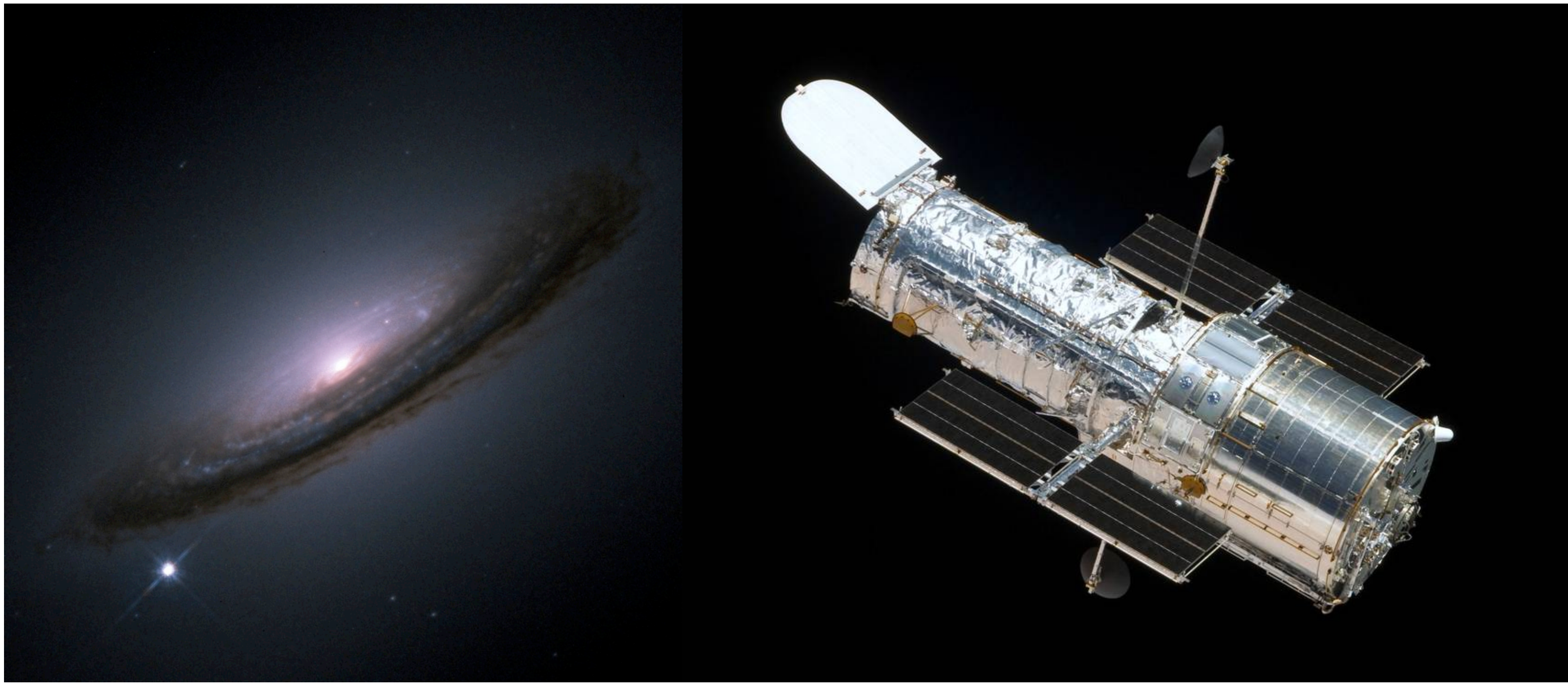

A. Riess, L. Macri, S. Casertano, D. Scolnic, A. Filippenko,
W. Yuan, S. Hoffman, …

SH0ES

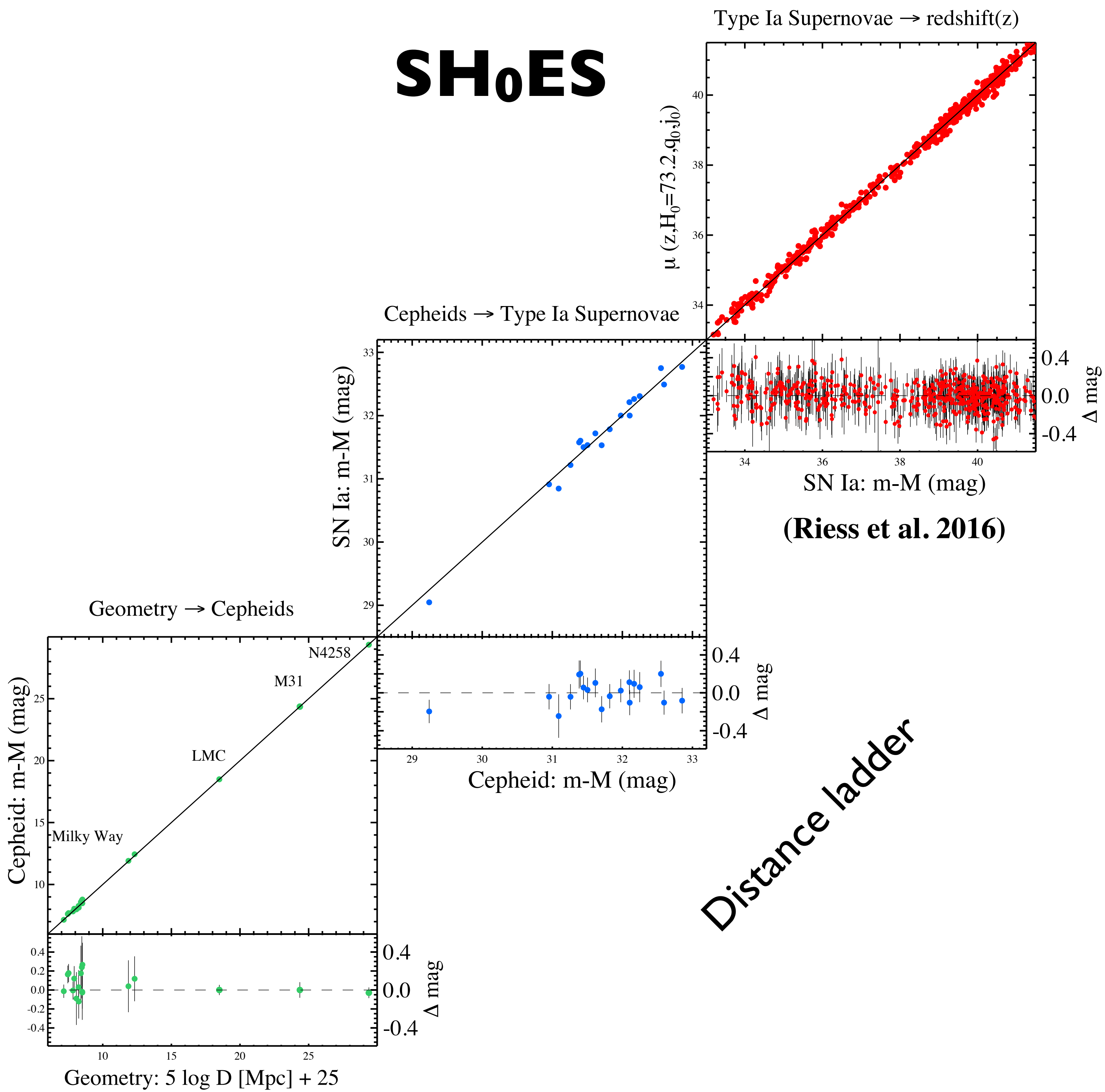

(Riess et al. 2016)

Distance ladder

SH$_0$ES

For example, with 4 distance anchors, 19 SNe Ia calibrated with Cepheids, 300 SNe at $z<0.15$

Riess et al. 2016 $H_0 = 73.24 \pm 1.74\,\mathrm{km\,s^{-1}\,Mpc^{-1}}$

with 7 additional long-period Cepheids in Milky Way

Riess et al. 2018 $H_0 = 73.48 \pm 1.66\,\mathrm{km\,s^{-1}\,Mpc^{-1}}$

and with 70 additional Cepheids in LMC

Riess et al. 2019 $H_0 = 74.03 \pm 1.42\,\mathrm{km\,s^{-1}\,Mpc^{-1}}$

just under 5σ from Planck 2018 TTTEEE+lowE+lensing

SH₀ES

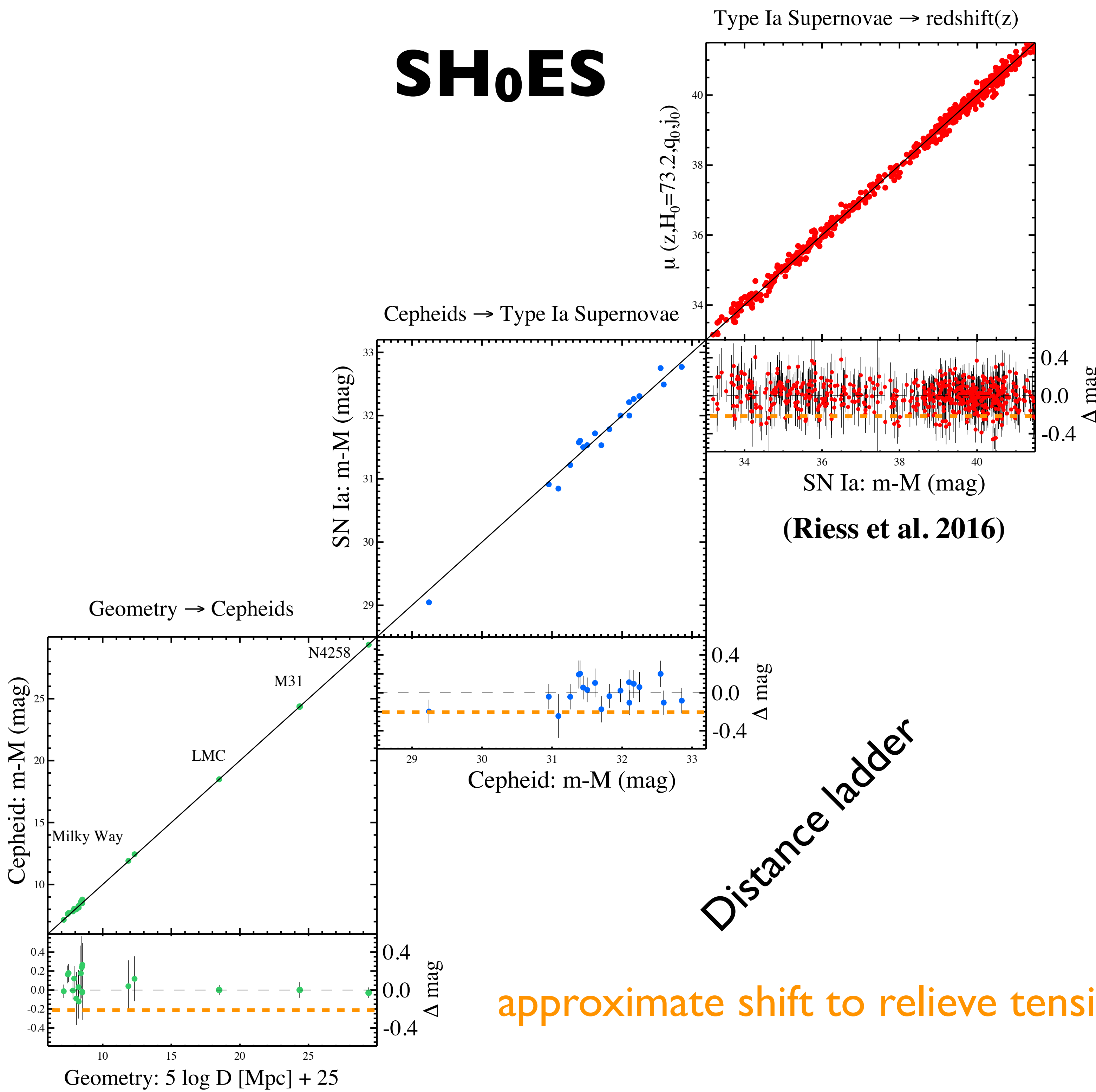

(Riess et al. 2016)

Distance ladder

approximate shift to relieve tension

WMAP, ACT, and SPT

Hinshaw et al. 2013

Planck 2013 XVI

Spergel, Flauger, Hlozek 2013

Planck 2015 XIII

Planck 2018 VI

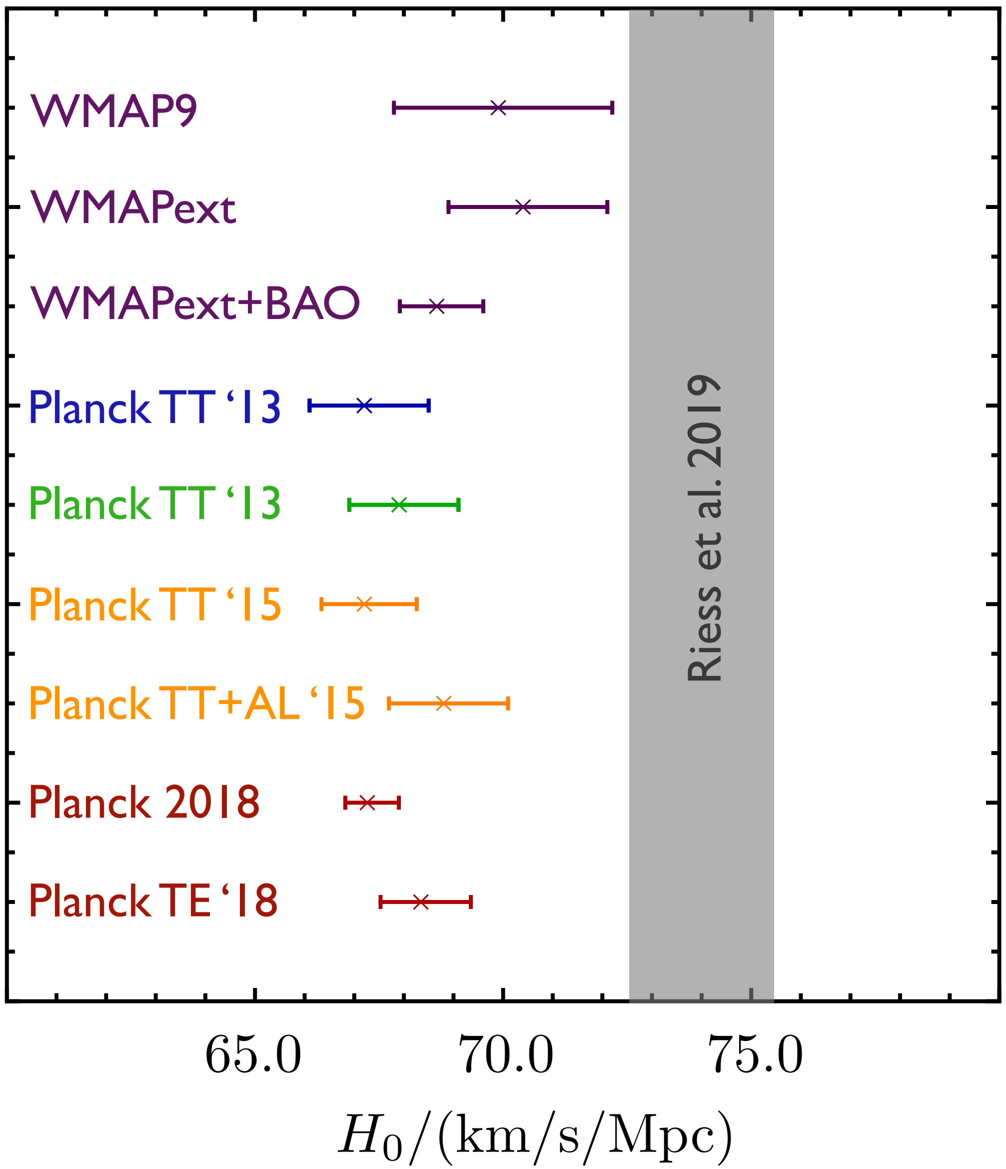

WMAP vs Planck

- Planck and WMAP temperature data agree very well at WMAP resolution

WMAP 94 GHz

Planck 100 GHz

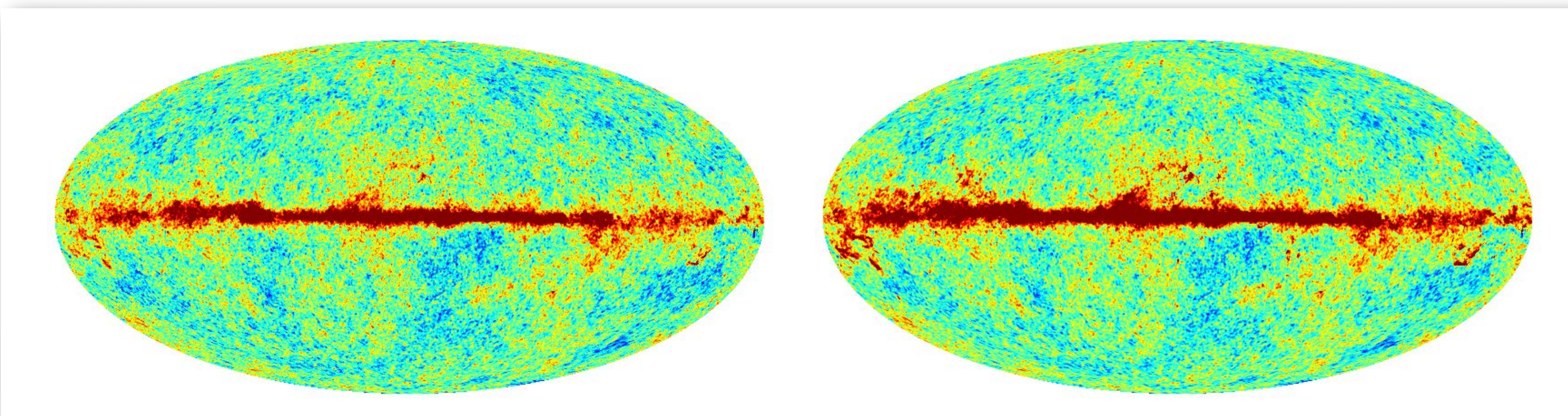

(N_{side}=512)

WMAP vs Planck

- Planck and WMAP temperature data agree very well at WMAP resolution
- Planck is much more powerful

WMAP 94 GHz

Planck 100 GHz

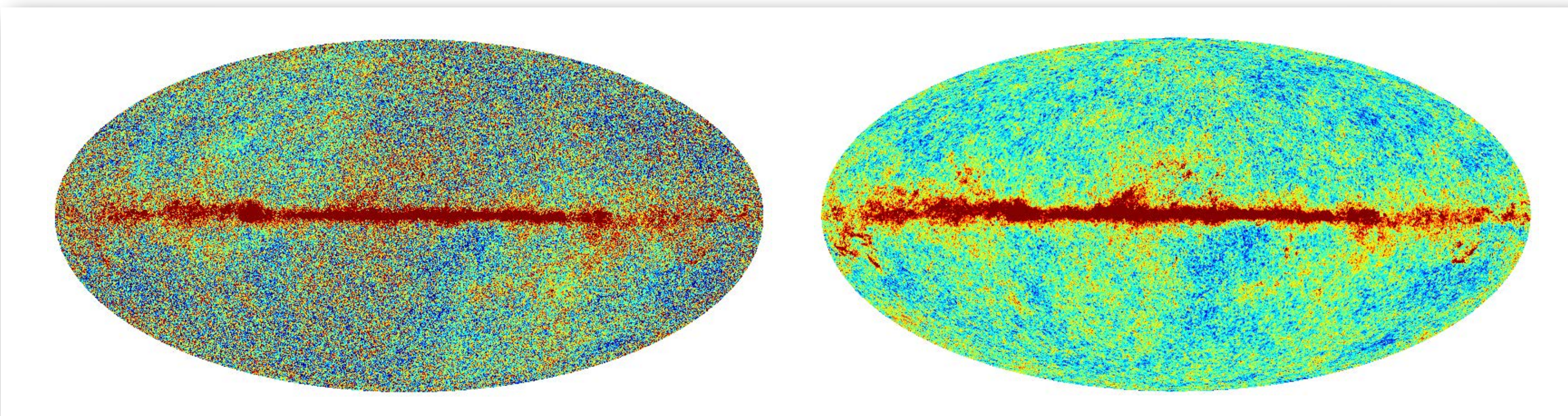

(N_{side}=1024)

Limited multipole ranges

Hinshaw et al. 2013

Planck 2018 VI

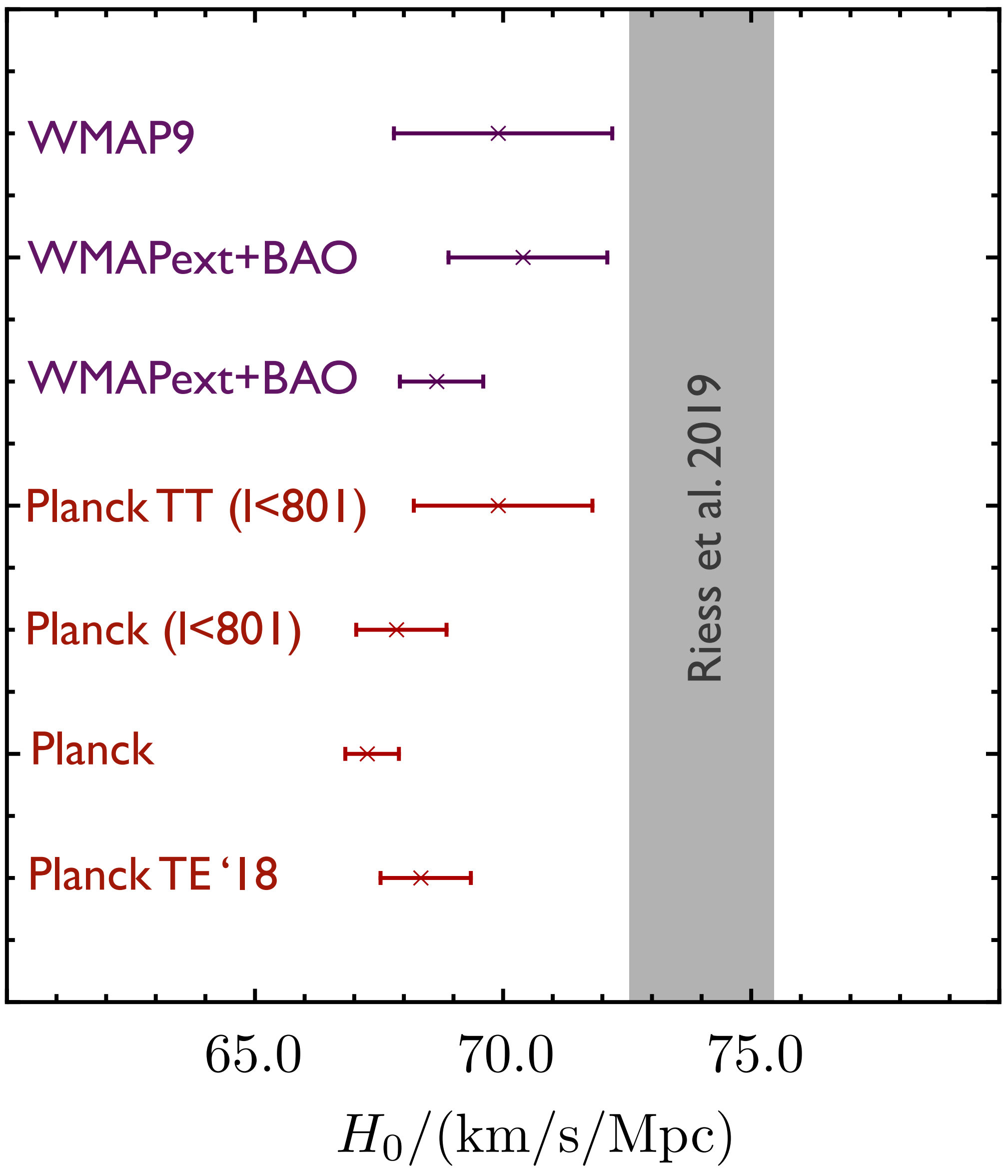

H_0 from the CMB

The CMB has limited sensitivity to the present expansion rate.

Approximating the baryon-photon plasma as a viscous fluid, and assuming a flat FLRW background, we schematically have

$$C_{TT,\ell} \simeq 4\pi T_{CMB}^2 \int_0^\infty \frac{dk}{k} \Delta_{\mathcal{R}}^2(k) e^{-2\tau} \times \left\{ \left[R_L - \frac{e^{-\int_0^{t_L} dt\, \Gamma(k,t)}}{(1+R_L)^{1/4}} \cos(kr_\star) \right] j_\ell(kD_M(z_L)) + \left[\frac{\sqrt{3} e^{-\int_0^{t_L} dt\, \Gamma(k,t)}}{(1+R_L)^{3/4}} \sin(kr_\star) \right] j_\ell'(kD_M(z_L)) \right\}^2$$

H_0 from the CMB

with comoving sound horizon

$$r_\star = \int_0^{t_L} \frac{c_s dt}{a(t)} \quad \text{where} \quad c_s = \frac{1}{\sqrt{3(1+R)}} \,, \; R = \frac{3\rho_b}{4\rho_\gamma}$$

and comoving angular distance to the last-scattering surface

$$D_M(z_L) = \int_{t_L}^{t_0} \frac{dt}{a(t)}$$

The k-integral is dominated by $k \approx \ell / D_M(z_L)$. So the peak positions are determined by the angular size of the sound horizon

$$\theta_\star = \frac{r_\star}{D_M(z_L)}$$

H_0 from the CMB

The temperature of the medium sets the photon energy density

$$\Omega_\gamma h^2 = 2.4729(2) \times 10^{-5} \qquad \text{(from FIRAS)}$$

Cold dark matter and baryon densities are measured relative to the photon energy density.

So the CMB anisotropies provide tight constraints on

$\theta_\star$	acoustic angular scale at last scattering
$\Delta^2_{\mathcal{R}}(k)$	usually parameterized through $A_{\rm s}, n_{\rm s}$
$\Omega_b h^2$	baryon density
$\Omega_c h^2$	dark matter density
τ	optical depth (through polarization)

H_0 from the CMB

which are the parameters that are reported*

Parameter	TT,TE,EE+lowE+lensing 68% limits
$\Omega_b h^2$	0.02237 ± 0.00015
$\Omega_c h^2$	0.1200 ± 0.0012
$100\theta_{MC}$	1.04092 ± 0.00031
τ	0.0544 ± 0.0073
$\ln(10^{10} A_s)$	3.044 ± 0.014
n_s	0.9649 ± 0.0042

*for historic reasons $\theta_{\rm MC}$, an approximation to $\theta_\star$, is reported

These are not measured by SH0ES. So there is no direct discrepancy between measurements.

H_0 from the CMB

Other parameters, like the Hubble parameter, can be "derived" from the CMB observations assuming a model

E.g. , in LCDM $\theta_\star(h, \Omega_m h^2, \Omega_b h^2)$ can be solved for h

Parameter	TT,TE,EE+lowE+lensing 68% limits
$\Omega_b h^2$	0.02237 ± 0.00015
$\Omega_c h^2$	0.1200 ± 0.0012
$100\theta_{MC}$	1.04092 ± 0.00031
τ	0.0544 ± 0.0073
$\ln(10^{10} A_s)$	3.044 ± 0.014
n_s	0.9649 ± 0.0042
H_0 [km s^{-1} Mpc^{-1}] . .	67.36 ± 0.54
Ω_Λ	0.6847 ± 0.0073
Ω_m	0.3153 ± 0.0073

H_0 from the CMB

Dependence on Hubble parameter

The sound horizon is essentially independent of h

$$r_\star(\Omega_m h^2, \Omega_b h^2, \ldots)$$

other parameters characterizing the early universe, $N_{\rm eff}$, ...

The comoving angular diameter distance depends on h

$$D_M(h, \Omega_m h^2, \Omega_b h^2, \ldots)$$

other parameters characterizing the late universe, Ω_K, w,...

Low redshift data

Ignoring all other data, we could easily reconcile the two data sets by changing the evolution of the universe after recombination.

However, LCDM with parameters as measured by Planck is in remarkable agreement with low-redshift large scale structure and supernova data

(Betoule et al. 2014)

(Anderson et al. 2013)

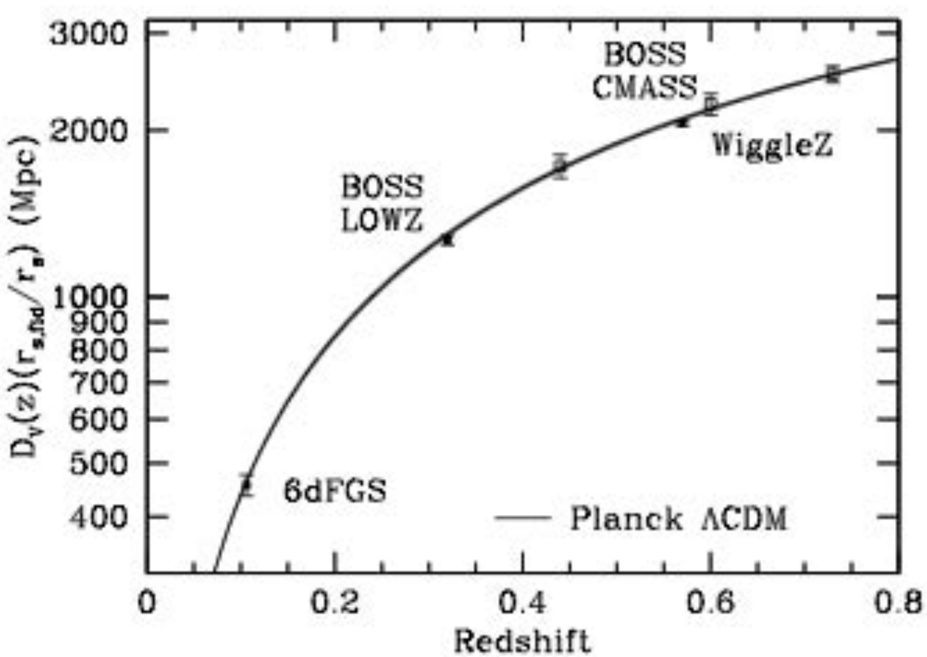

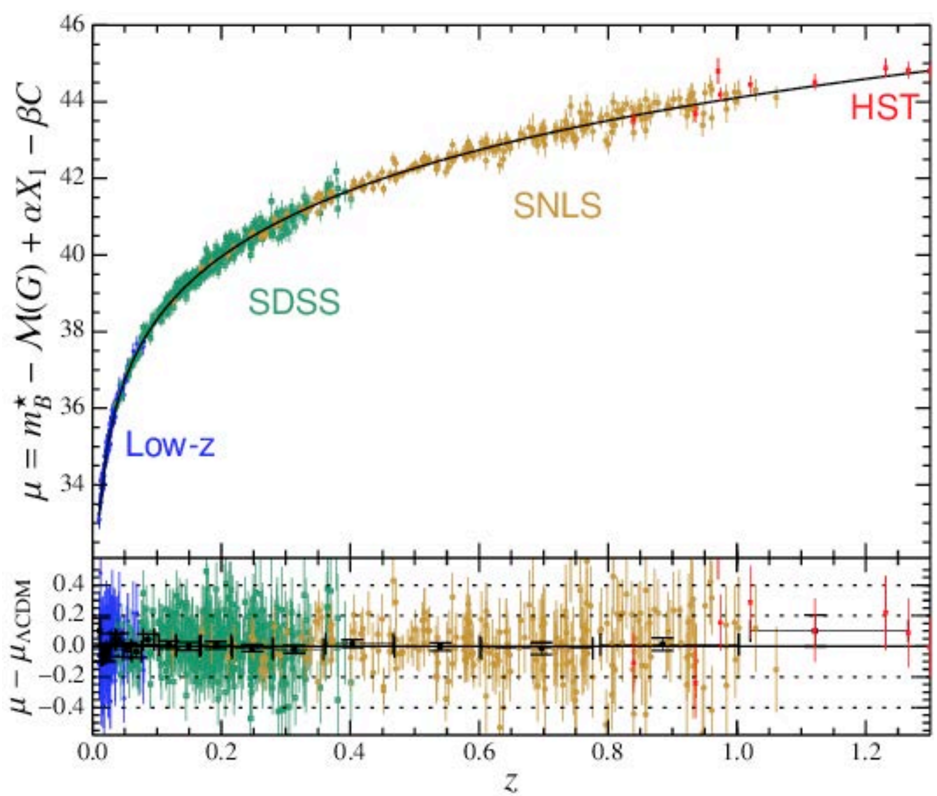

Baryon Acoustic Oscillations

(Almost) the same acoustic scale we saw in the CMB is imprinted on the matter distribution.

(Alam et al. 2016)

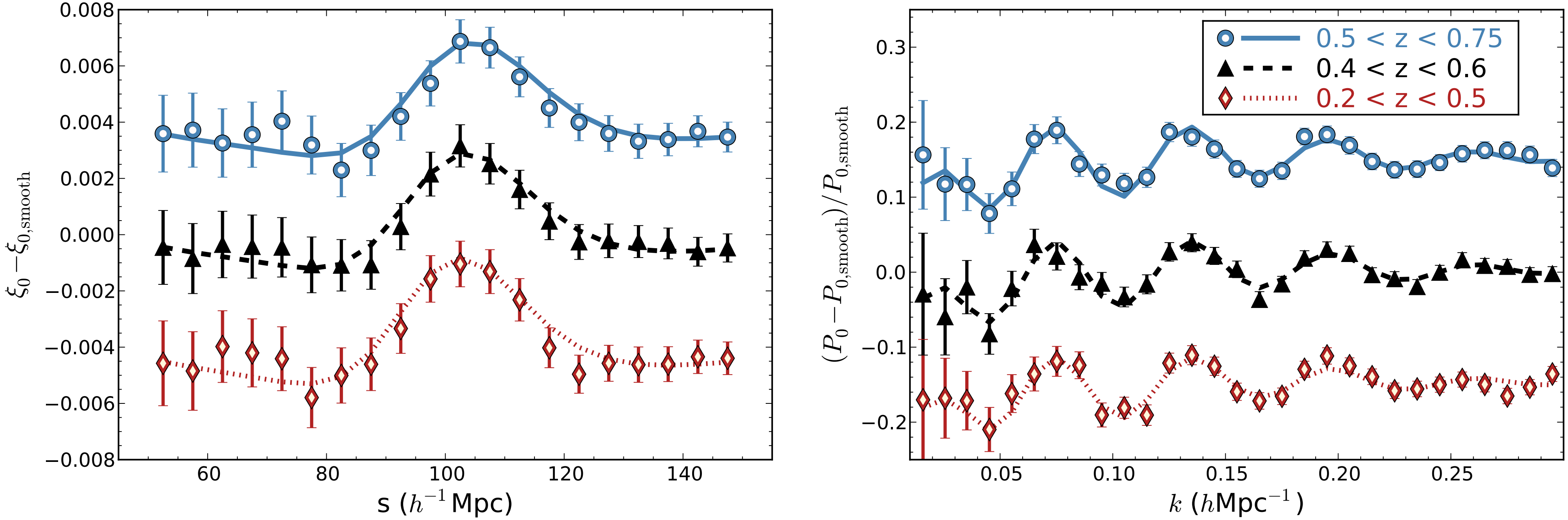

Baryon Acoustic Oscillations

In a given redshift bin, the feature will appear at an angular scale

$$\theta_d(z) = \frac{r_d}{D_M(z)}$$

where r_d is the sound horizon at the time baryons decouple

$$r_d = \int_0^{t_d} \frac{c_s dt}{a(t)}$$

and $D_M(z)$ is the comoving angular diameter distance to redshift z

We can predict these assuming LCDM with parameters determined by Planck and compare.

Baryon Acoustic Oscillations

Unlike the CMB, redshift surveys carry 3d information, and we can also use the radial information. The scale associated with the comoving sound horizon is

$$\Delta z(z) = H(z) r_d$$

These "anisotropic" BAO measurements agree with the Planck predictions

(Alam et al. 2016)

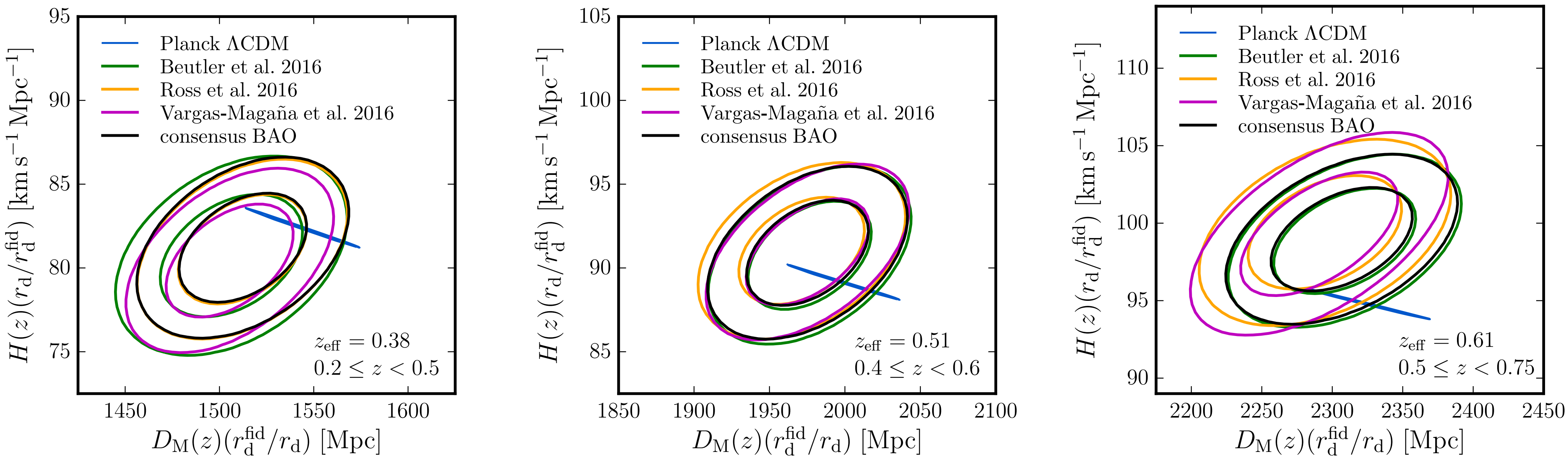

Baryon Acoustic Oscillations

It is also common to present results for "isotropic" BAO measurements

(Planck 2018 VI)

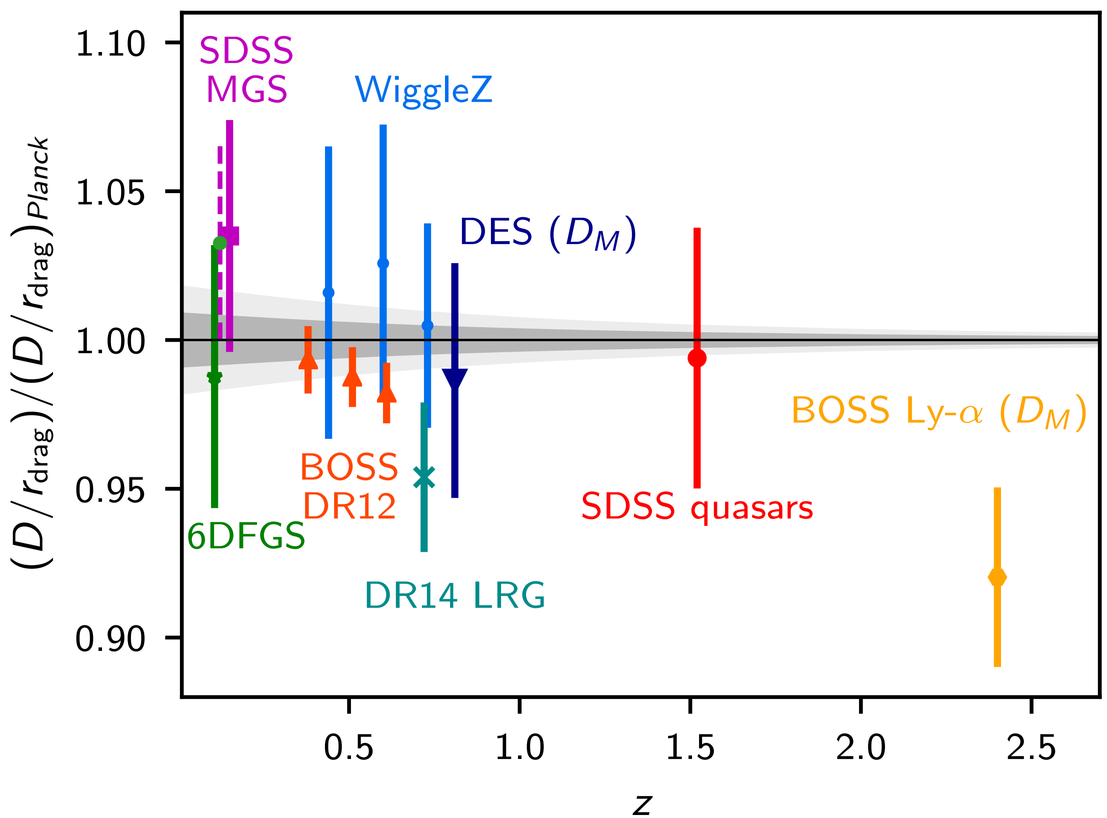

$D_V(z)/r_d$ with $D_V(z) = \left(D_M^2(z) \frac{z}{H(z)} \right)^{1/3}$

H_0 from BAO

We can use BAO data to predict H_0 within LCDM

Taking $\Omega_\gamma h^2$ as known (from FIRAS), we have

$$r_d(\Omega_m h^2, \Omega_b h^2) \text{ and } D_M(z, h, \Omega_m h^2, \Omega_b h^2)$$

With $\Omega_b h^2$ from primordial deuterium abundance, BAO data predict H_0

(Cuceu et al. 2019)

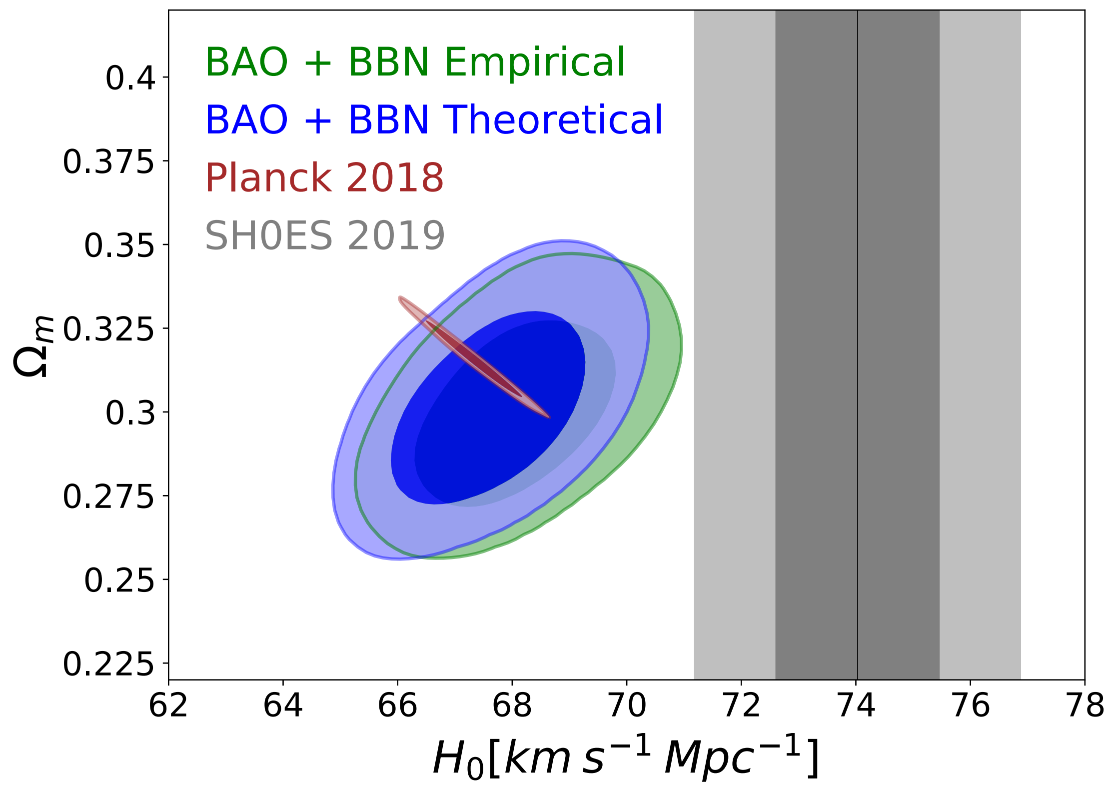

H_0 from BAO

Perhaps somewhat less convincing when broken up into galaxy and Lyα BAO

(Cuceu et al. 2019)

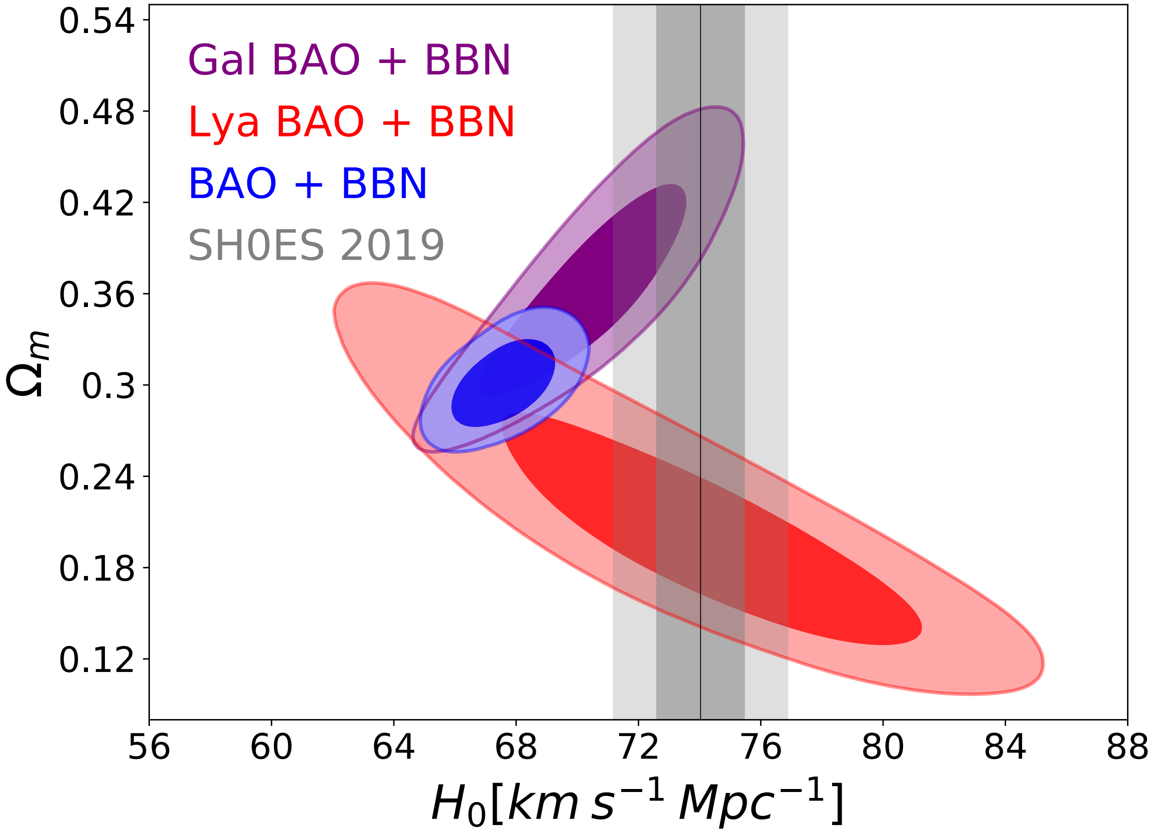

H_0 from LSS

A more ambitious approach includes the full shape information of the power spectrum, not only the baryon acoustic oscillations.

e.g. DES+BAO+BBN $H_0 = 67.2^{+1.2}_{-1.0}\,\mathrm{km\,s^{-1}\,Mpc^{-1}}$ **(Abbott et al. 2017)**

or based on final data from BOSS:

(Philcox et al. 2020)

	base $\nu\Lambda$CDM	
Parameter	FS	FS+BAO
ω_{cdm}	$0.1265^{+0.01}_{-0.01}$	$0.1259^{+0.009}_{-0.0093}$
n_s	$0.8791^{+0.081}_{-0.076}$	$0.9003^{+0.076}_{-0.071}$
H_0	$68.55^{+1.5}_{-1.5}$	$68.55^{+1.1}_{-1.1}$
σ_8	$0.7285^{+0.055}_{-0.053}$	$0.7492^{+0.053}_{-0.052}$
Ω_m	$0.3203^{+0.018}_{-0.019}$	$0.3189^{+0.015}_{-0.015}$

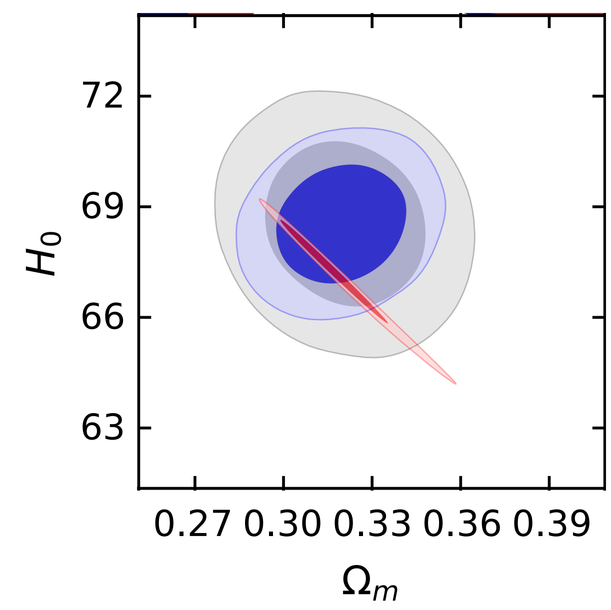

LCDM with parameters as inferred from the CMB is in remarkable agreement with large scale structure data.

Supernovae

Supernovae tightly constrain, and are consistent with LCDM as inferred from Planck to very low redshift

(Planck 2018 VI)

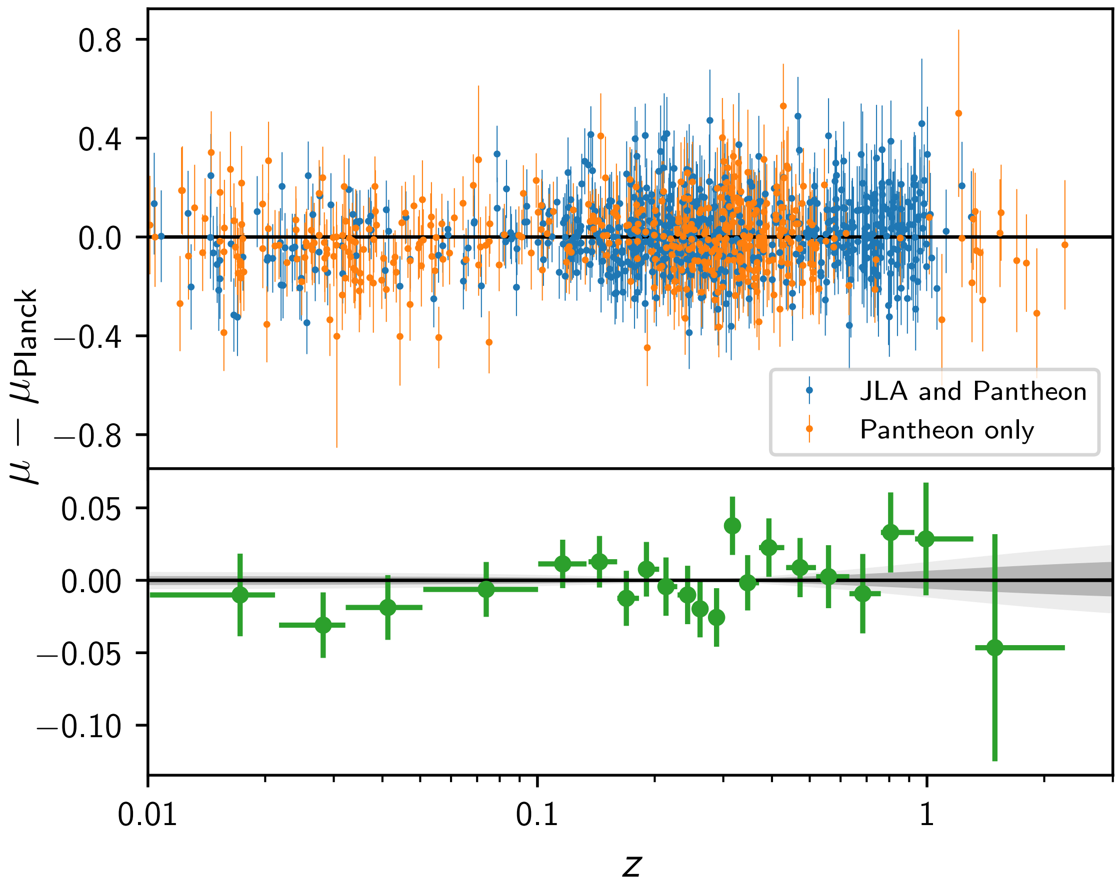

Early Universe

Our understanding of particle physics at high energies is incomplete.

So can't we easily resolve the tension by modifying the expansion history and hence the sound horizon at early times?

Our period of ignorance is remarkably short compared to the age of the universe at last scattering.

We need O(1) change to Hubble rate at $z \sim 10^4$ or O(10%) change at $z \sim 10^3$, i.e. at eV scales where we do think we know the field content.

Modes probed by CMB precisely enter the horizon at this time. Measurements tightly constrain any such modification and upcoming polarization experiments will significantly tighten these constraints.

Early Universe

Redshift at horizon entry

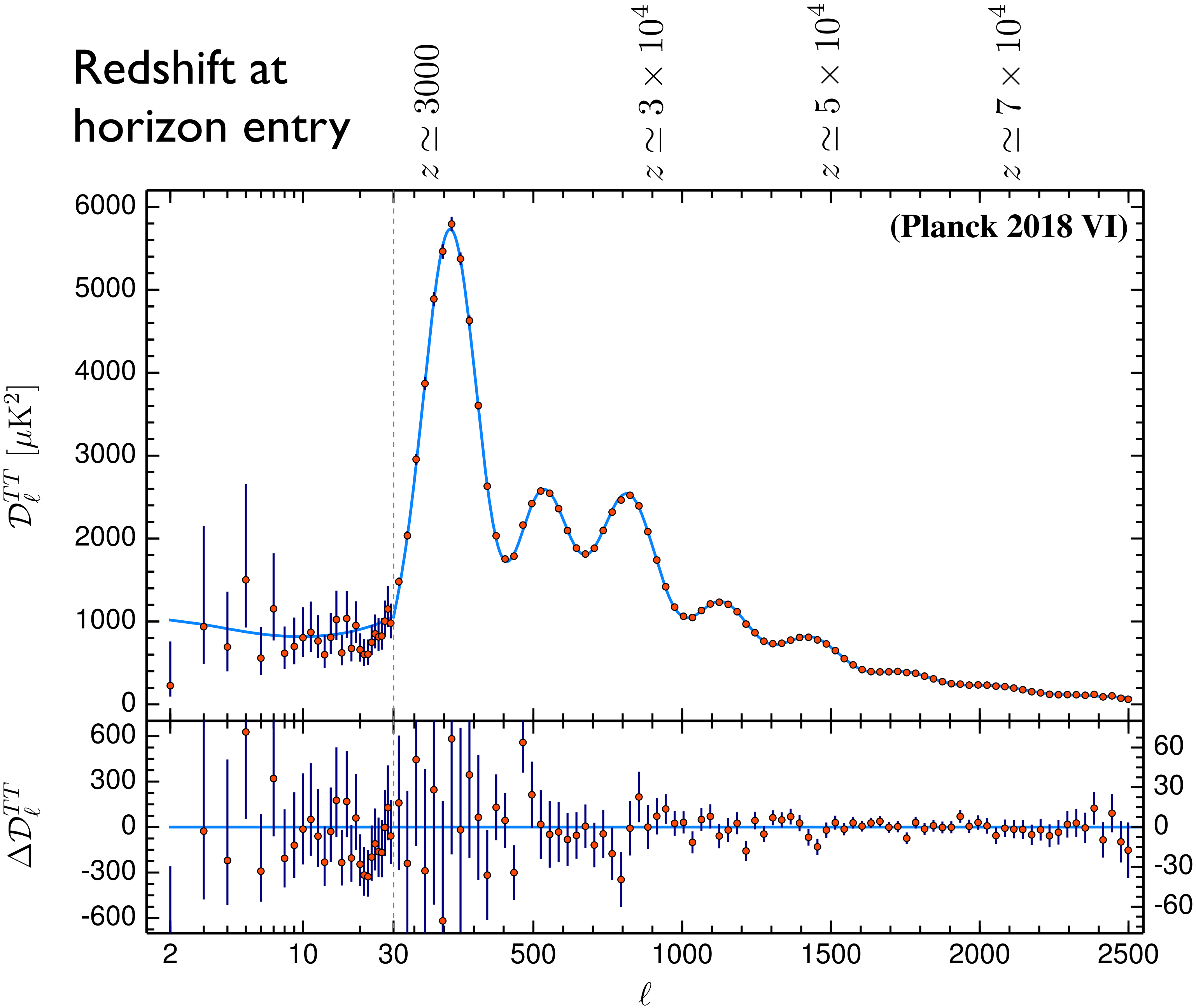

A Closer look at the distance ladder

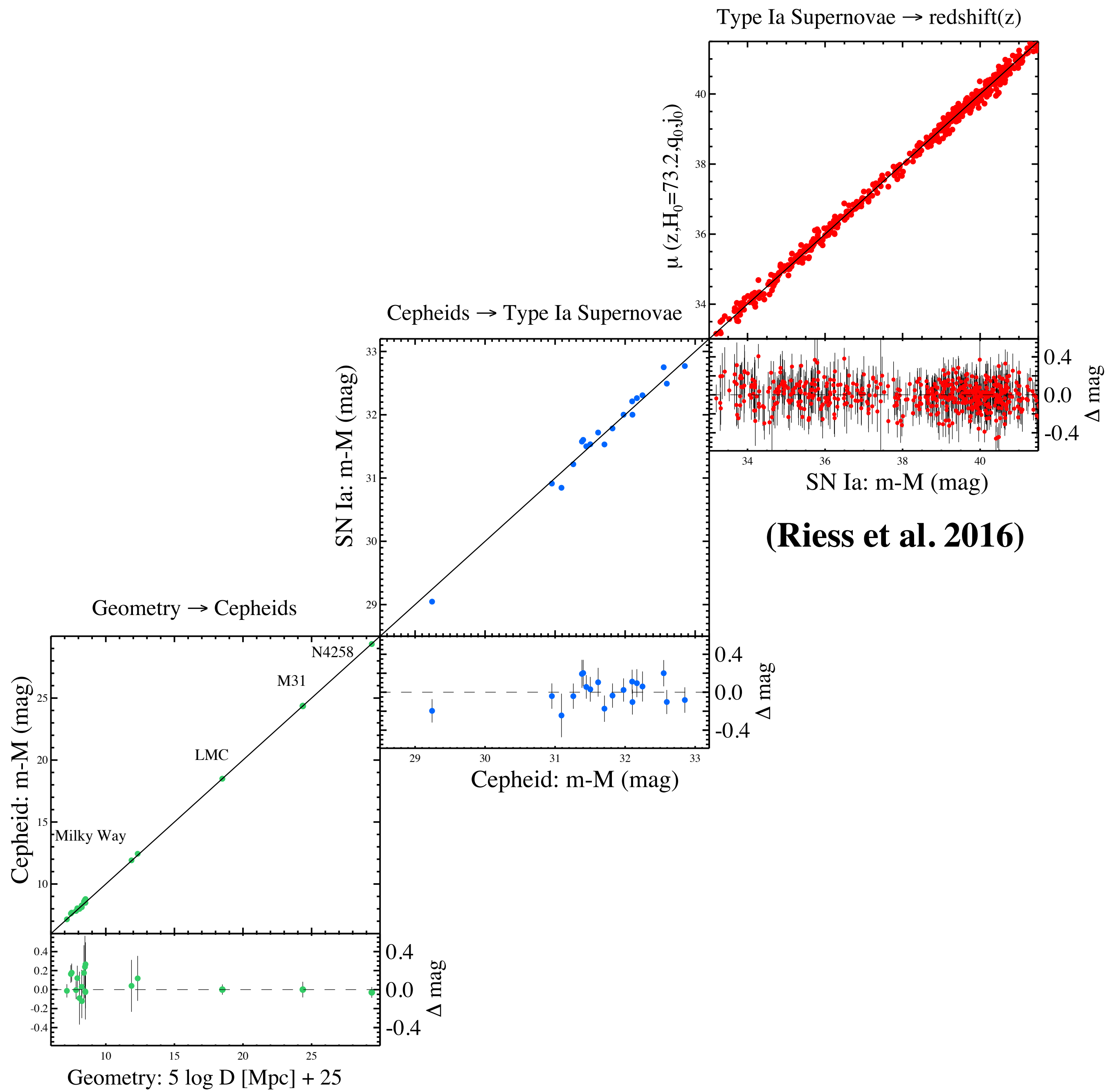

(Riess et al. 2016)

NGC 4258

NGC 4258

VLBI monitoring of megamaser emission in accretion disk

(Argon et el. 2007)

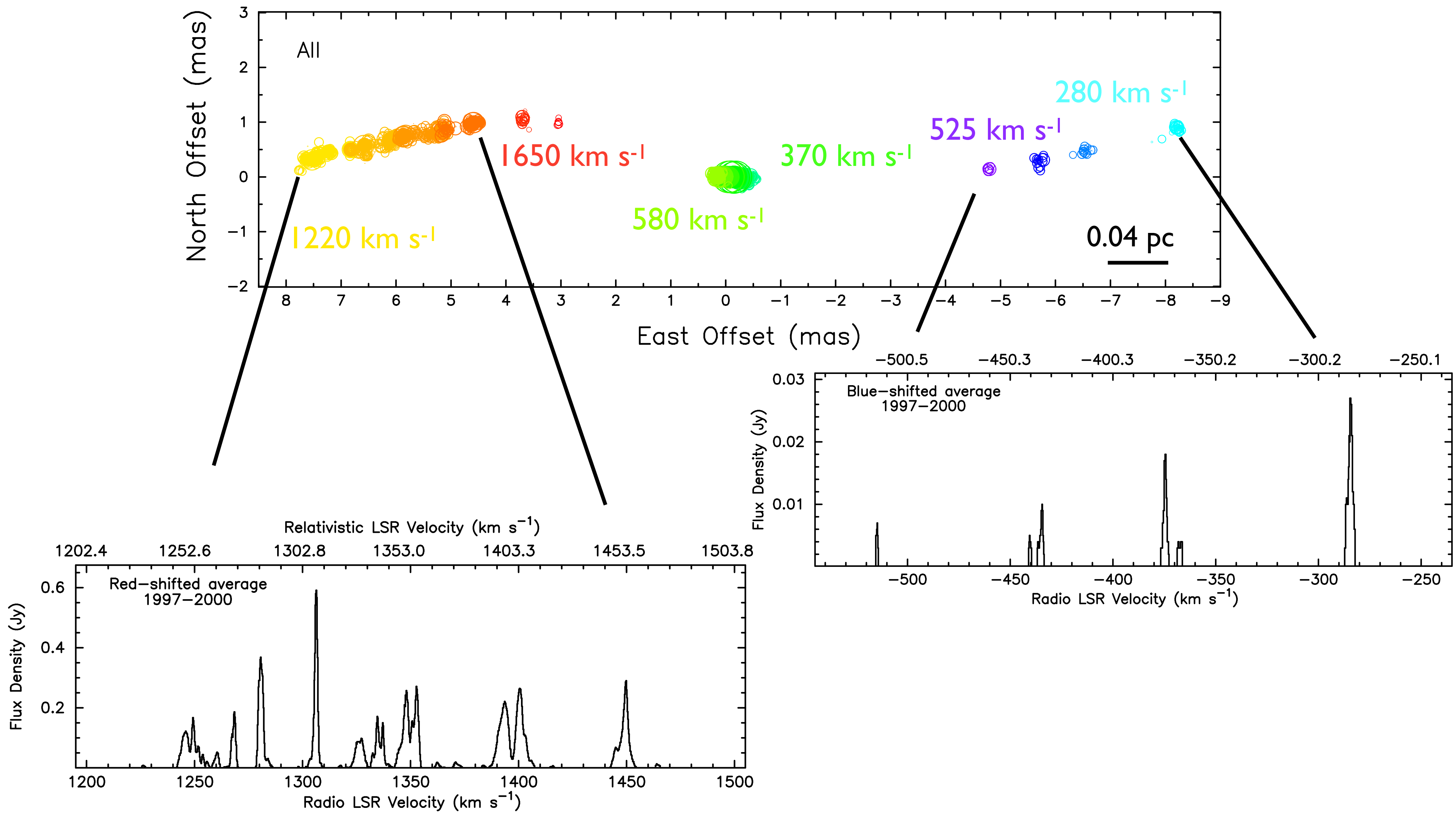

NGC 4258

(Argon et el. 2007)

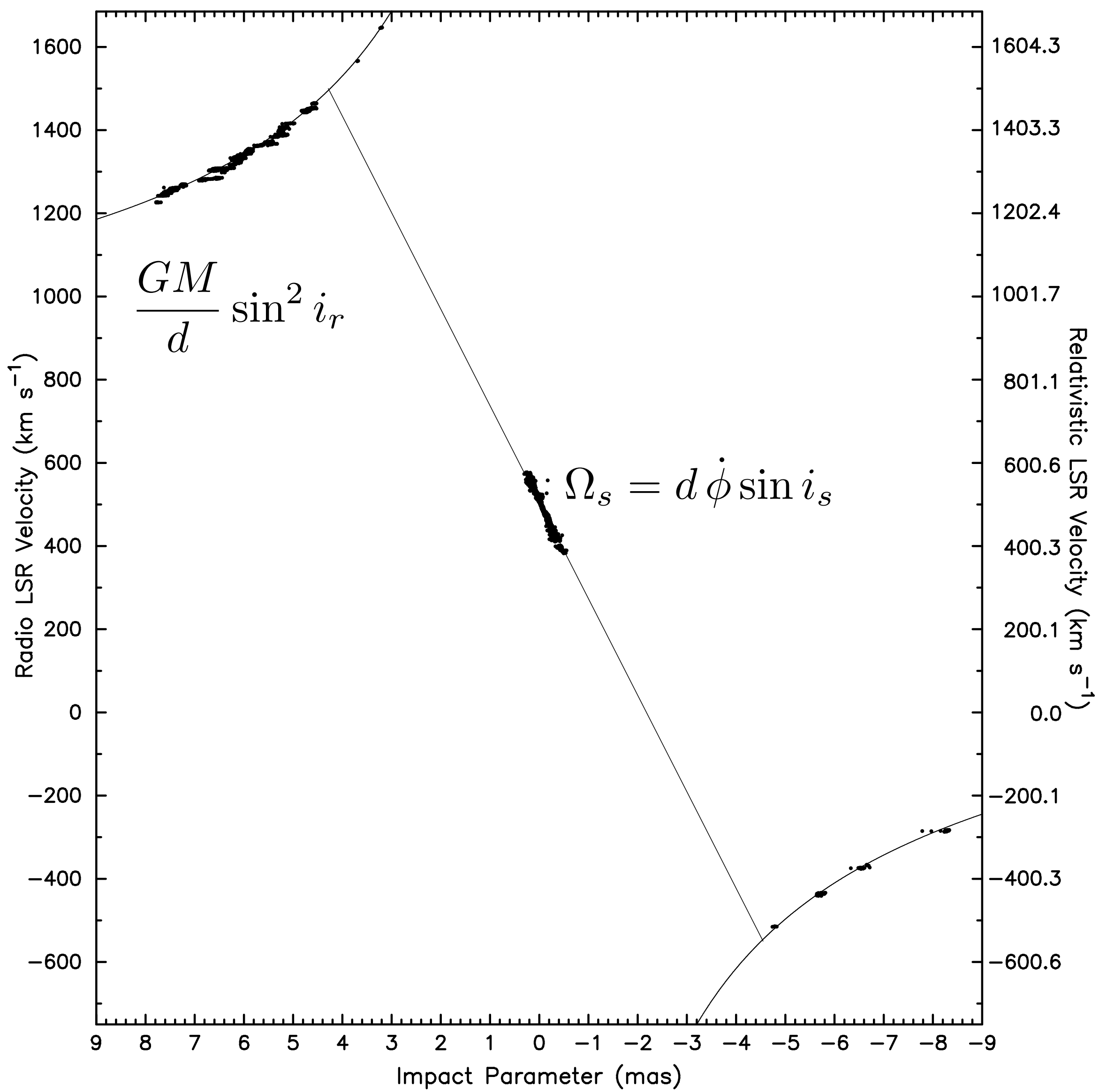

NGC 4258

VLBI monitoring at multiple epochs allows to measure accelerations an to infer the distance

From Physics I

$$\dot{v}_{\rm los} = \frac{1}{d}\Omega_s^{4/3}\left(\frac{GM}{d}\sin i_s\right)^{1/3}\frac{1}{\sin i_s}$$

This leads to

$$d = 7.576 \pm 0.082 \pm 0.076\,{\rm Mpc}$$ **(Reid et al. 2019)**

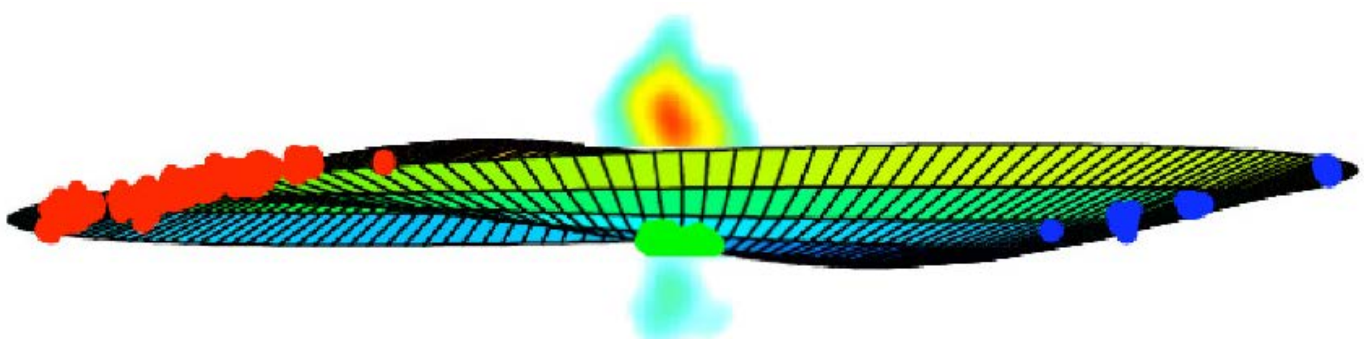

This can now be used to calibrate other distance indicators

Detached Eclipsing Binaries

Binary star systems with radii well inside their Roche surfaces

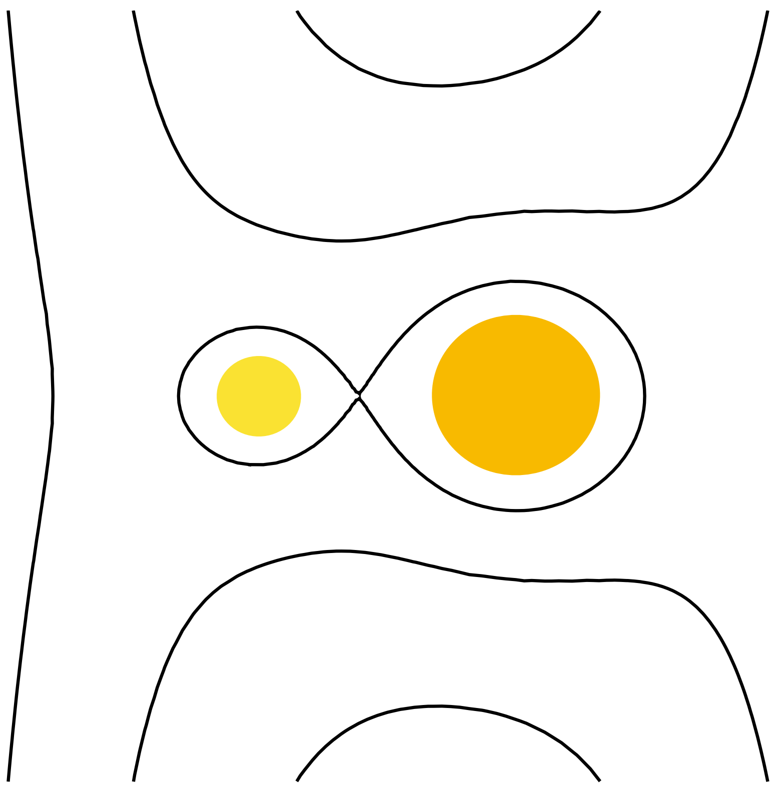

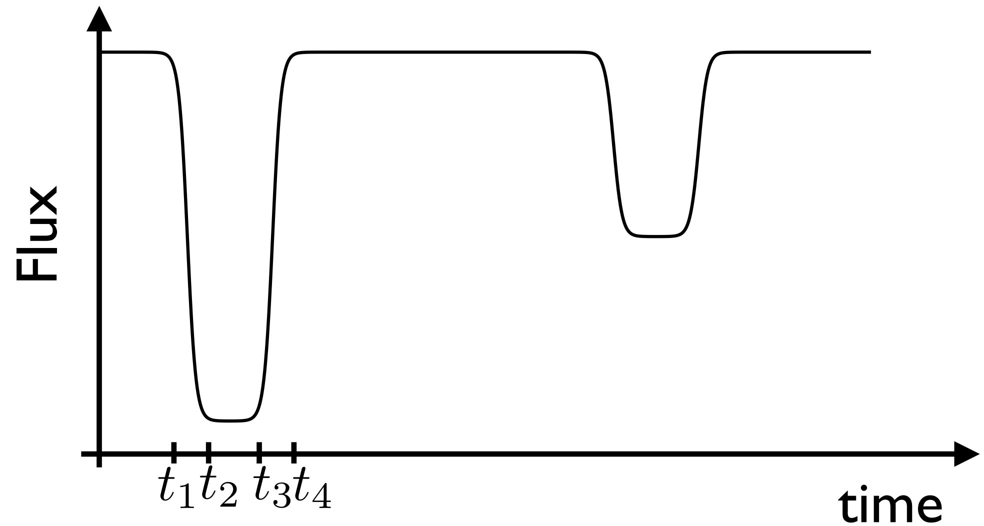

$$\frac{t_4 - t_1}{T} = \frac{2(r_1 + r_2)}{2\pi a}$$

$$\frac{t_3 - t_2}{T} = \frac{2(r_1 - r_2)}{2\pi a}$$

$$2\pi a = (v_1 + v_2)T$$

Light curves and radial velocities allow to infer the stellar radii

Detached Eclipsing Binaries

Detached eclipsing binaries in the LMC **(Graczyk et al. 2018)**

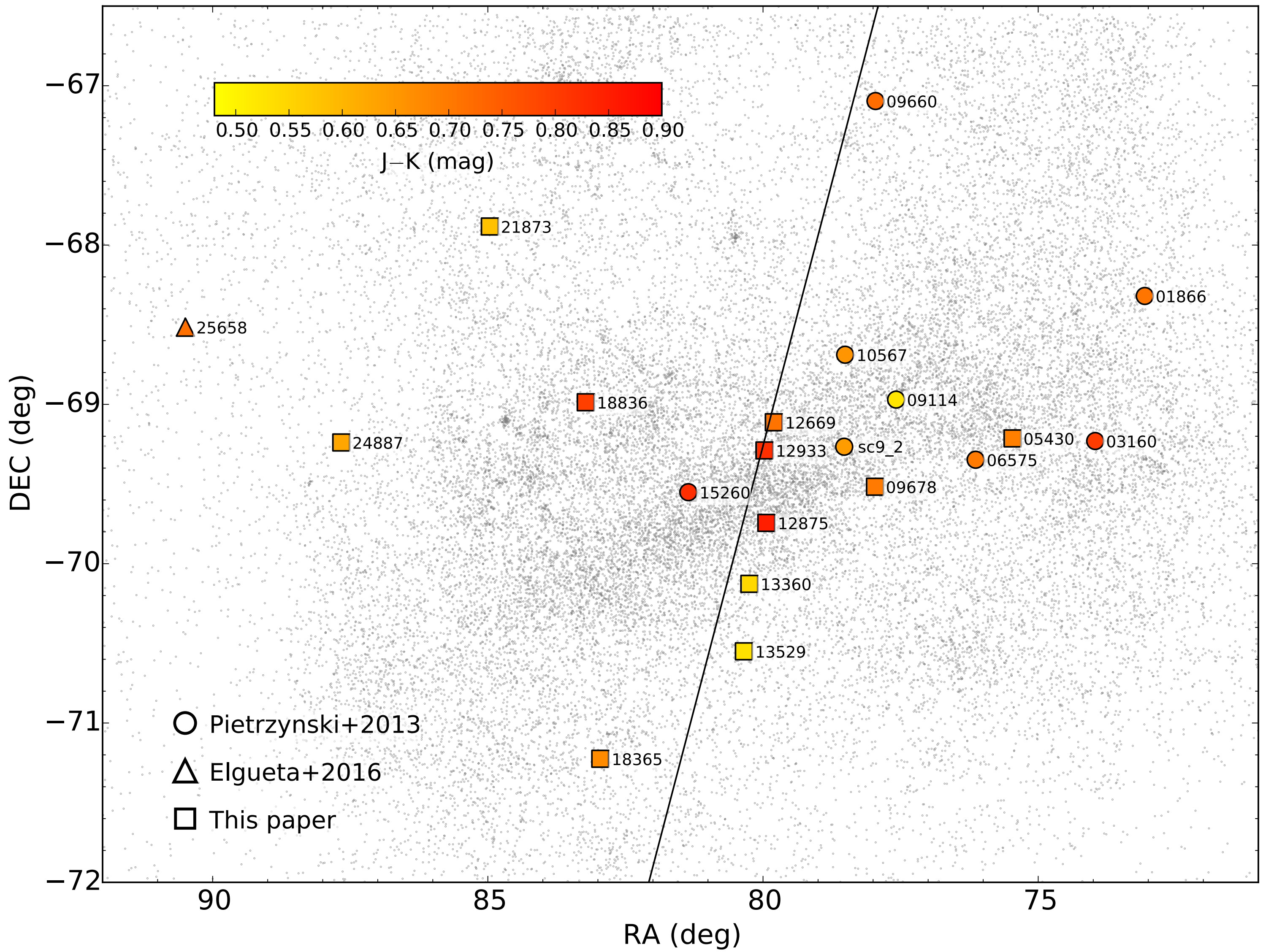

Detached Eclipsing Binaries

(Graczyk et al. 2018)

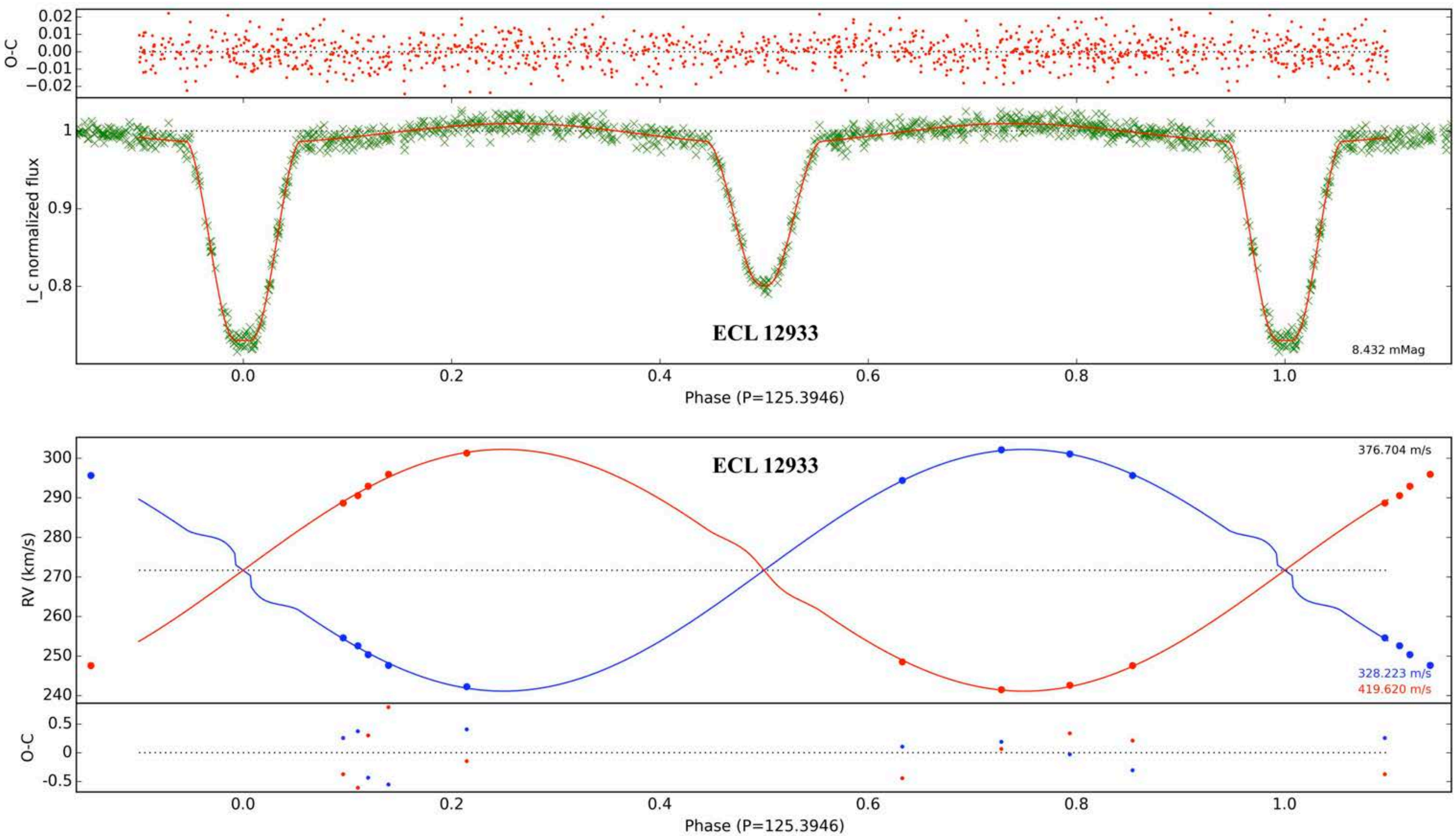

Detached Eclipsing Binaries

To measure the distance, we need the angular size.

For nearby stars angular sizes can be measured with interferometry. For baseline d and wave number k

$$V = \frac{1}{\bar{\bar{I}}} \int d^2\theta I(\theta) e^{ik\theta\cdot\mathbf{d}}$$

E.g. for uniform disk with angular diameter ϕ

$$V = \frac{2J_1(kd\,\phi/2)}{kd\,\phi/2}$$

For stars in the LMC, would require a baseline of $10^5\,\mathrm{km}$.

So the angular size is measured for similar nearby stars instead.

Detached Eclipsing Binaries

Only the first lobe of the visibility is measured. This implies no information about limb darkening is available.

Either uniform disk radii are converted using stellar atmosphere models, or predictions based on stellar atmosphere are fit directly.

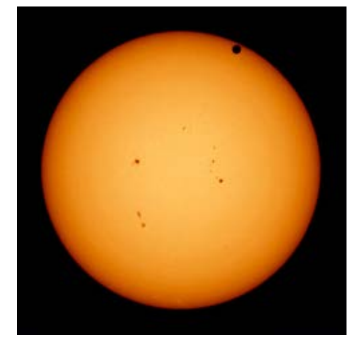

(Nordgren et al. 2001) ANGULAR DIAMETERS FROM THE NPOI AND MARK III

HR No. (1)	Spec. Type (2)	N_i (3)	NPOI θ_U (mas) (4)	LDC_N (5)	NPOI θ_L (mas) (6)	LDC_M (7)	MrkIII θ_L (mas) (8)
165	K3III	4	3.94 ± 0.04	1.076	4.24 ± 0.06	1.071	4.17 ± 0.06
168	K0IIIa	7	5.29 ± 0.05	1.068	5.65 ± 0.08	1.064	5.72 ± 0.08
617	K2IIIab	17	6.47 ± 0.03	1.073	6.94 ± 0.08	1.068	6.84 ± 0.10

This leads to a 5-10% correction to diameter, depending on the star and observing frequency.

Detached Eclipsing Binaries

From angular sizes of nearby stars to angular sizes in the LMC

For stars with known distance and and limb-darkened angular diameters, we can define the surface brightness

$$S_V = V_0 + 5\log(\phi)$$

with reddening corrected magnitude V_0

For late type stars this tightly correlates with color

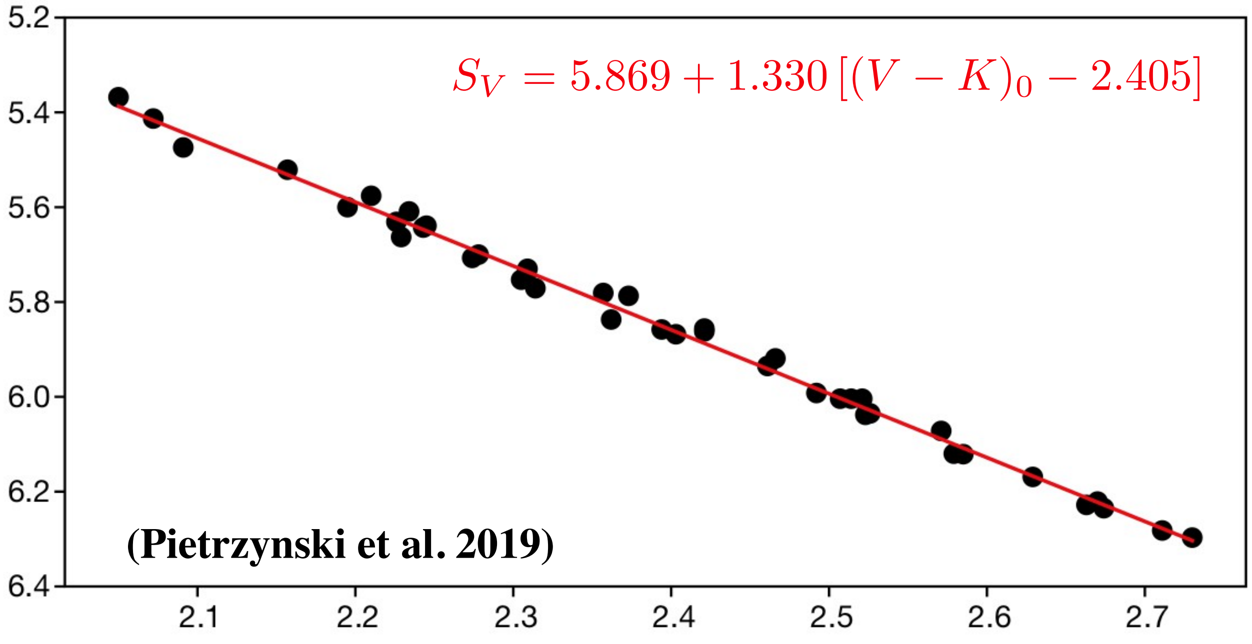

Detached Eclipsing Binaries

So the angular diameter is inferred from

$$\phi[\text{mas}] = 10^{\frac{1}{5}(S_V((V-K)_0)-V_0)}$$

and the distance is

$$d = \frac{2R}{\phi}$$

Distance to LMC from 20 detached eclipsing binaries

$$d = 49.59 \pm 0.09 \pm 0.54\,\text{kpc}$$ **(Pietrzynski et al. 2019)**

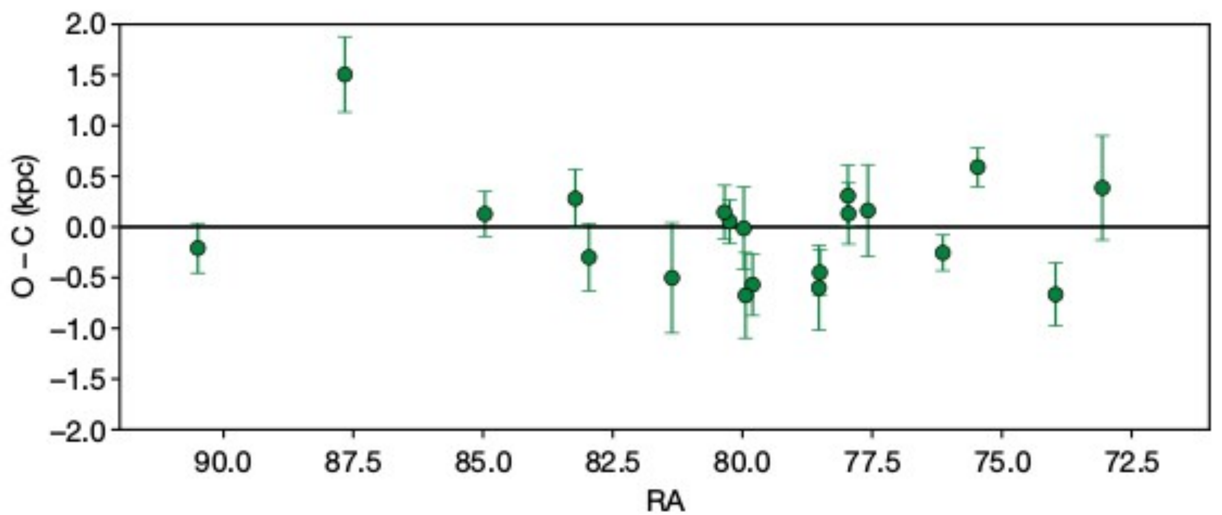

Cepheids in the distance anchors

Given the distance measurements, we can calibrate the Cepheid period luminosity relation (accounting for extinction)

$$m = a \log P + b$$

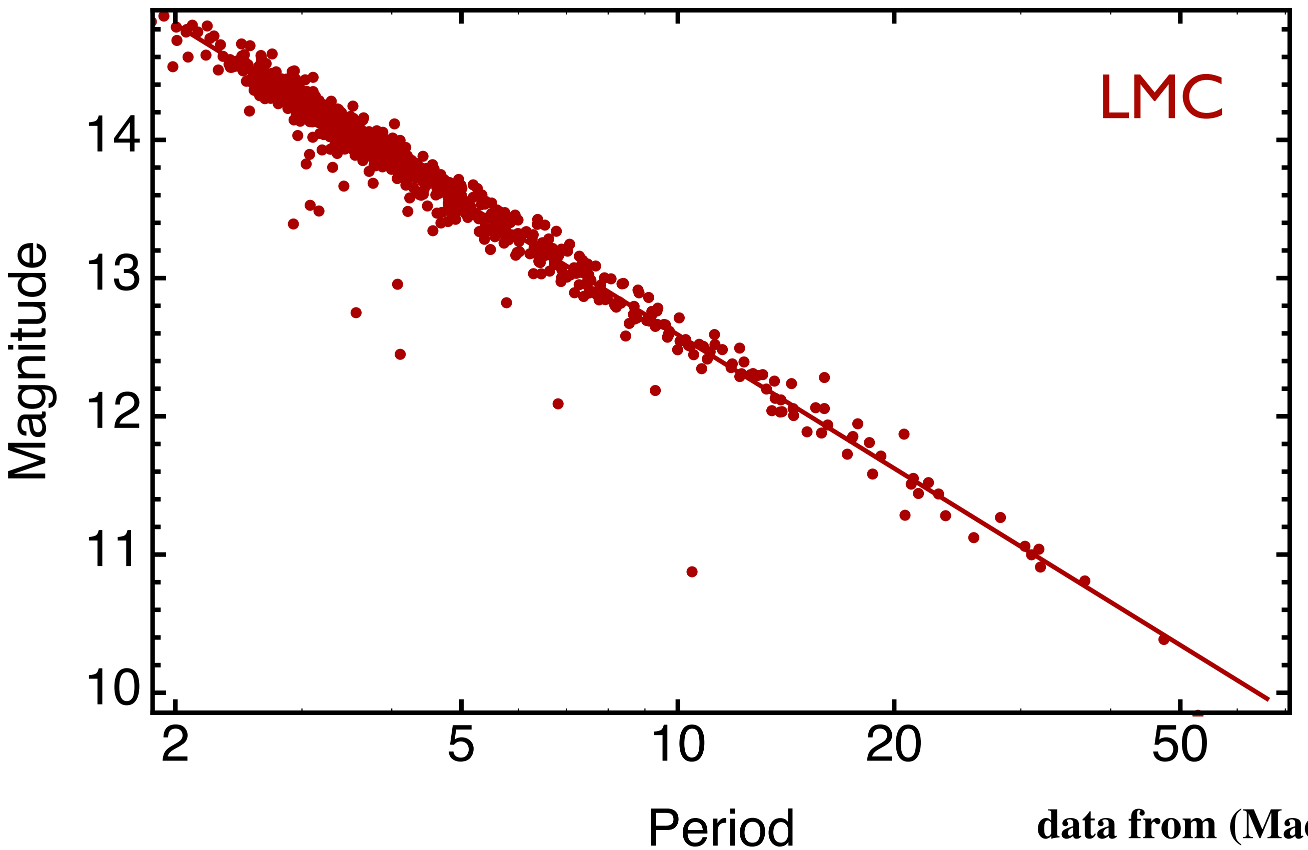

data from (Macri et al. 2015)

Cepheids in the distance anchors

Given the distance measurements, we can calibrate the Cepheid period luminosity relation (accounting for extinction)

$$m = a \log P + b$$

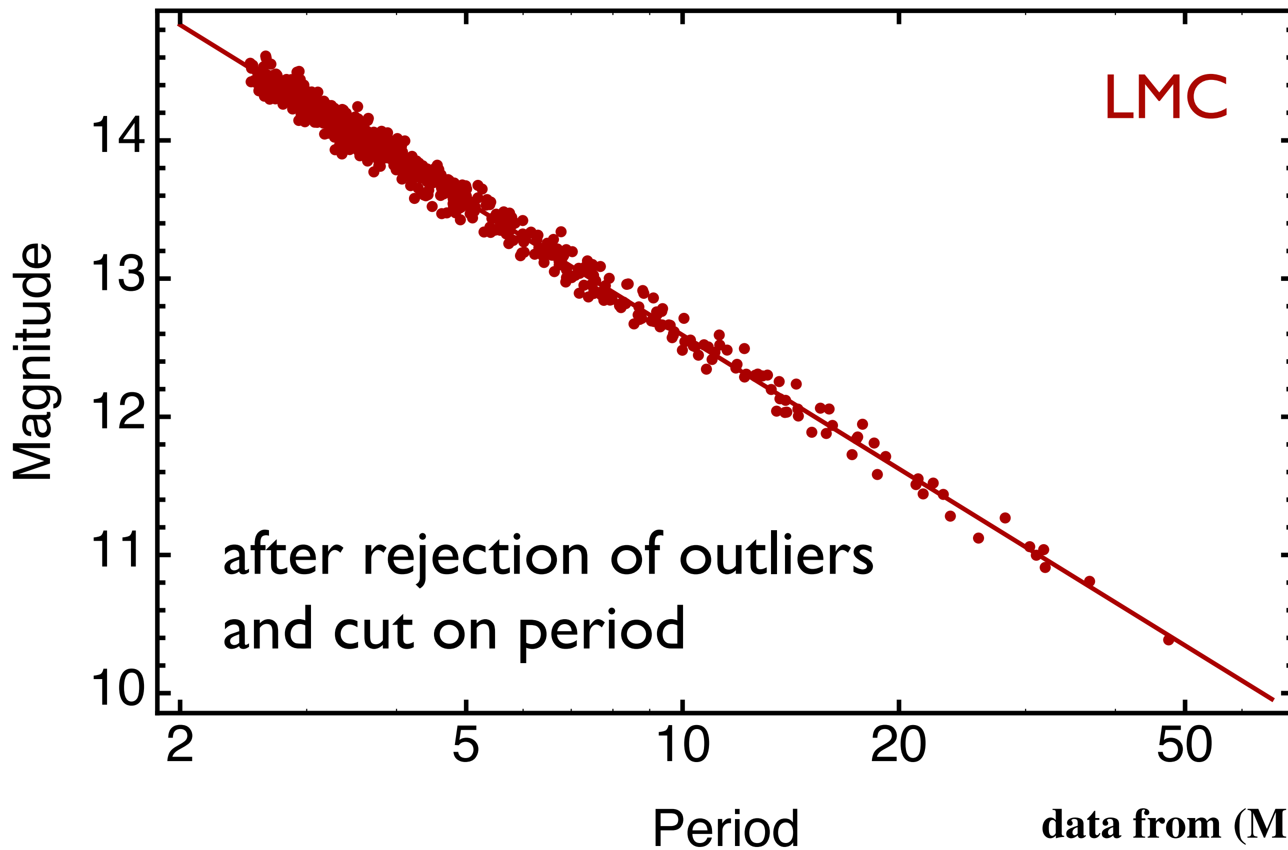

data from (Macri et al. 2015)

Dispersion much larger than measurement errors and "intrinsic scatter" is added in the fits

Cepheids in SNIe hosts

With the absolute calibration of the Cepheids, we can calibrate the distances to the supernova hosts

(Riess et al. 2016)

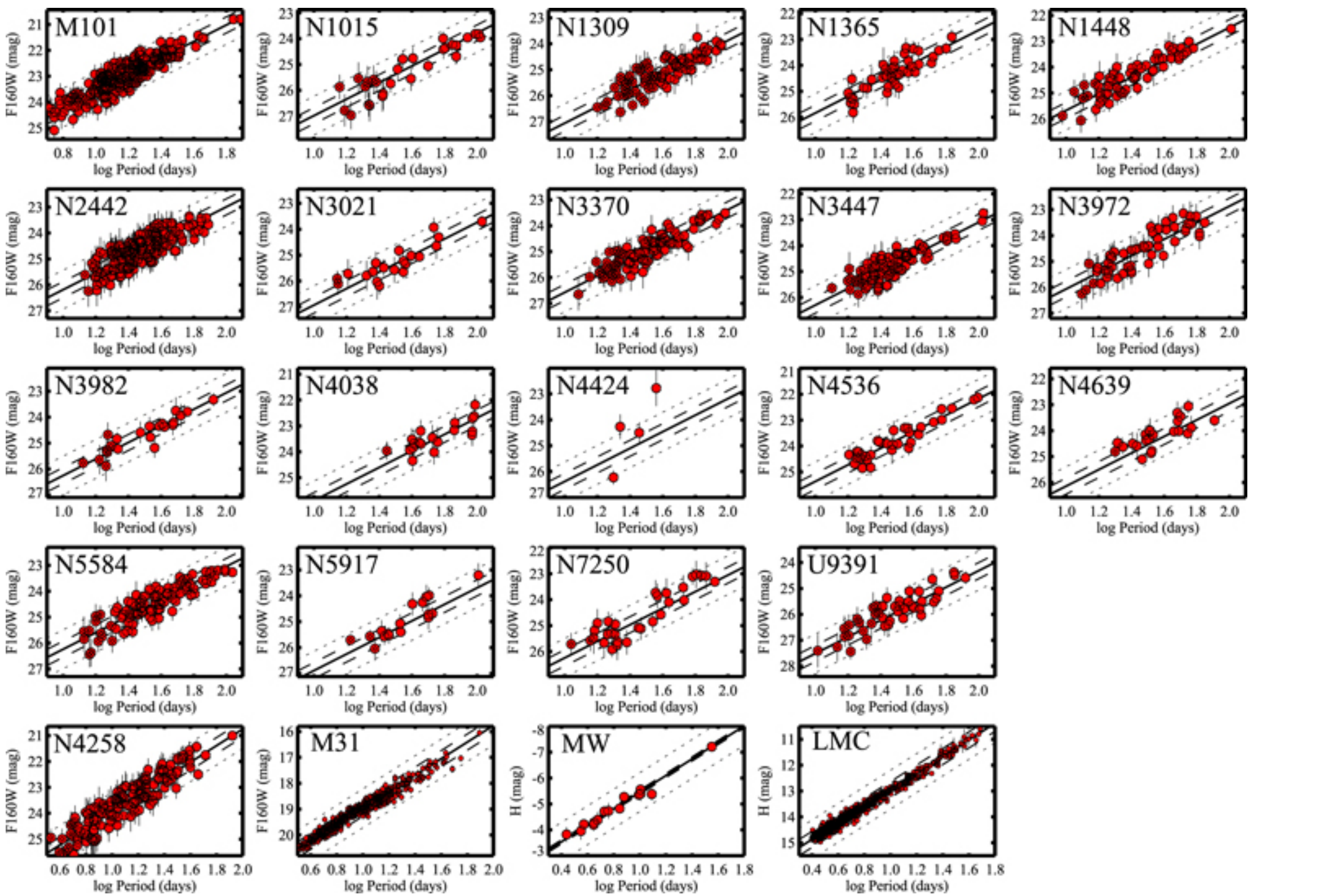

$$m_{H\,i,j}^{W} = (\mu_{0,i} - \mu_{0,N4258}) + zp_{W,N4238} + b_W \log P_{i,j} + Z_W \Delta \log(O/H)_{i,j}$$

Supernovae in SNIe hosts

This allows to calibrate the absolute supernova magnitude

from Cepheids

$$m^0_{B,i} = (\mu_{0,i} - \mu_{0,N4258}) + m^0_{B,N4258}$$

from supernova lightcurve fitting

$$m_{B,i} = m^0_{B,i} + \alpha x_1 - \beta c$$

stretch and color corrections

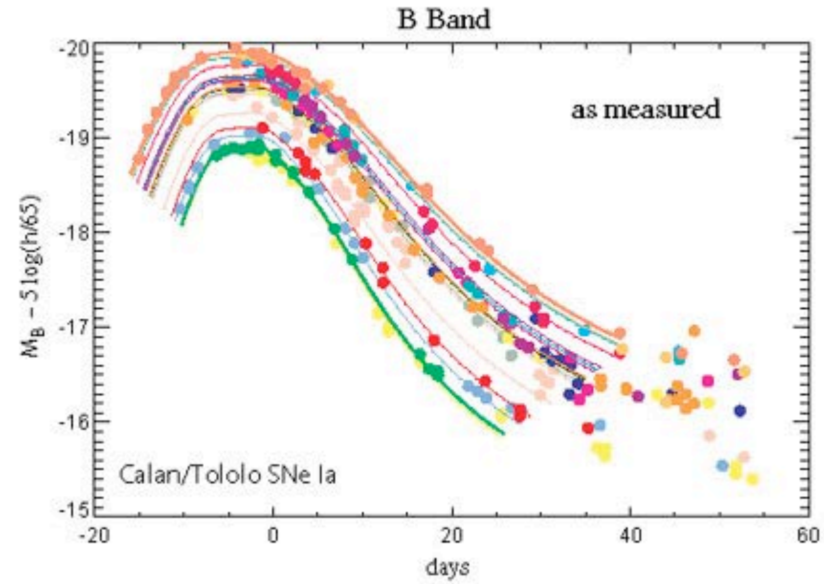

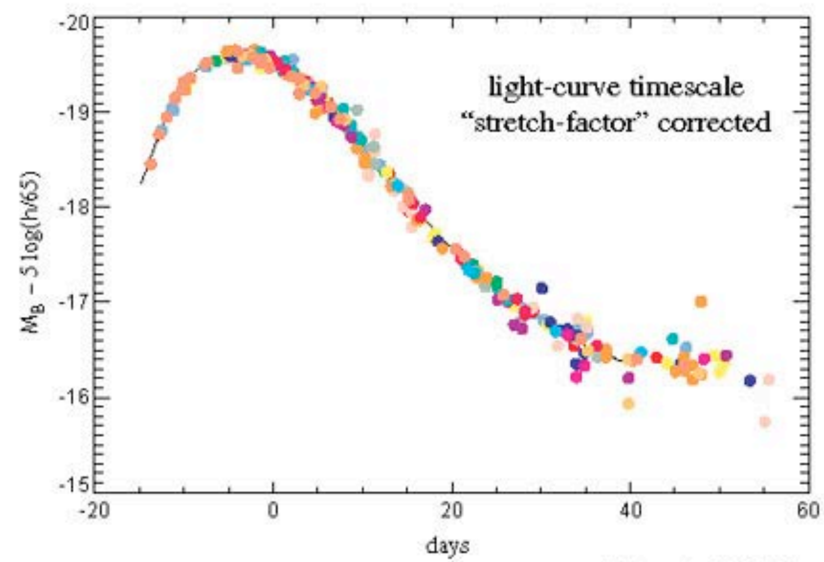

Kim, *et al.* (1997)

Supernovae

Once calibrated, supernovae are used to measure H_0

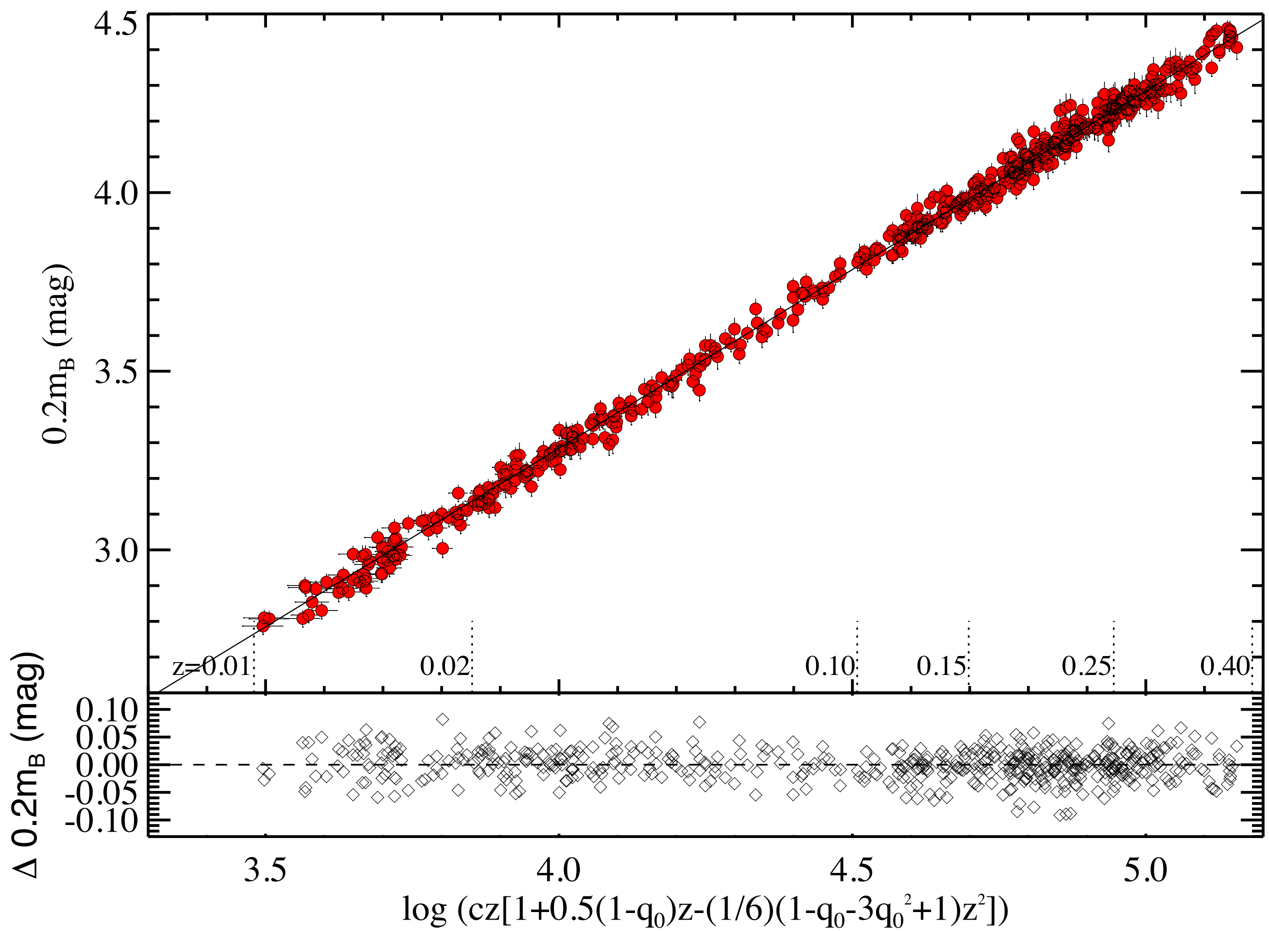

$$\log H_0 = \frac{(m^0_{B,N4258} - \mu_{0,N4258}) + 5a_x + 25}{5}$$

Cepheids in anchors and SNIe hosts

Note that the anchors are dominated by short period Cepheids whereas hosts are dominated by long period Cepheids

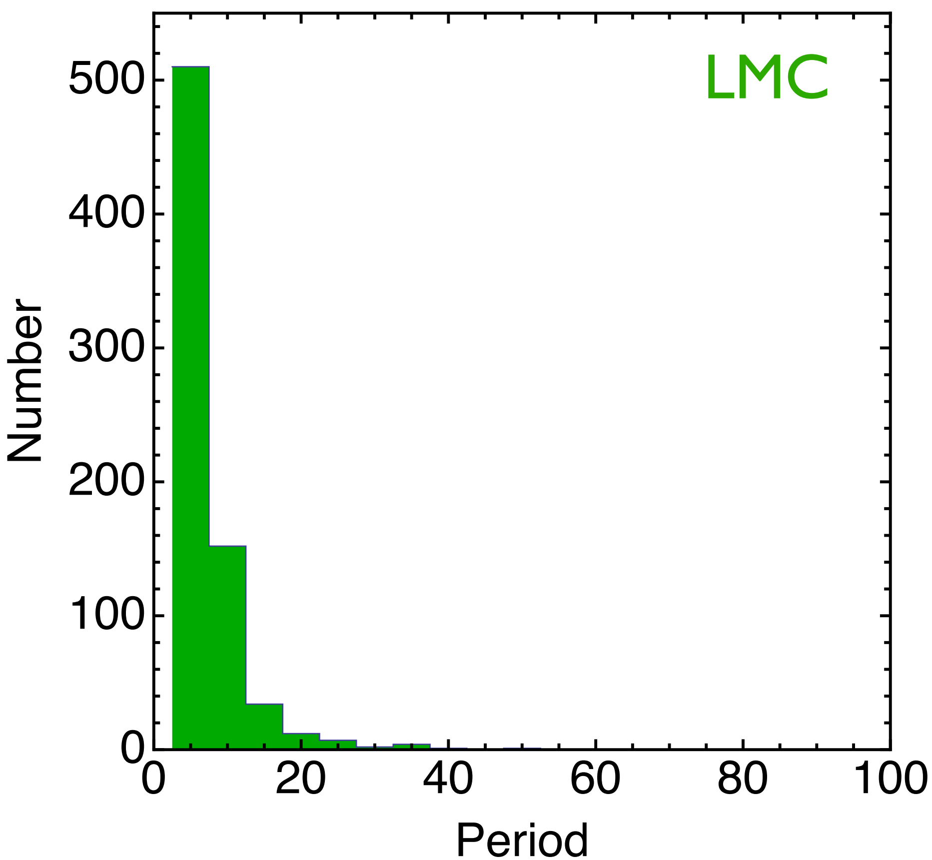

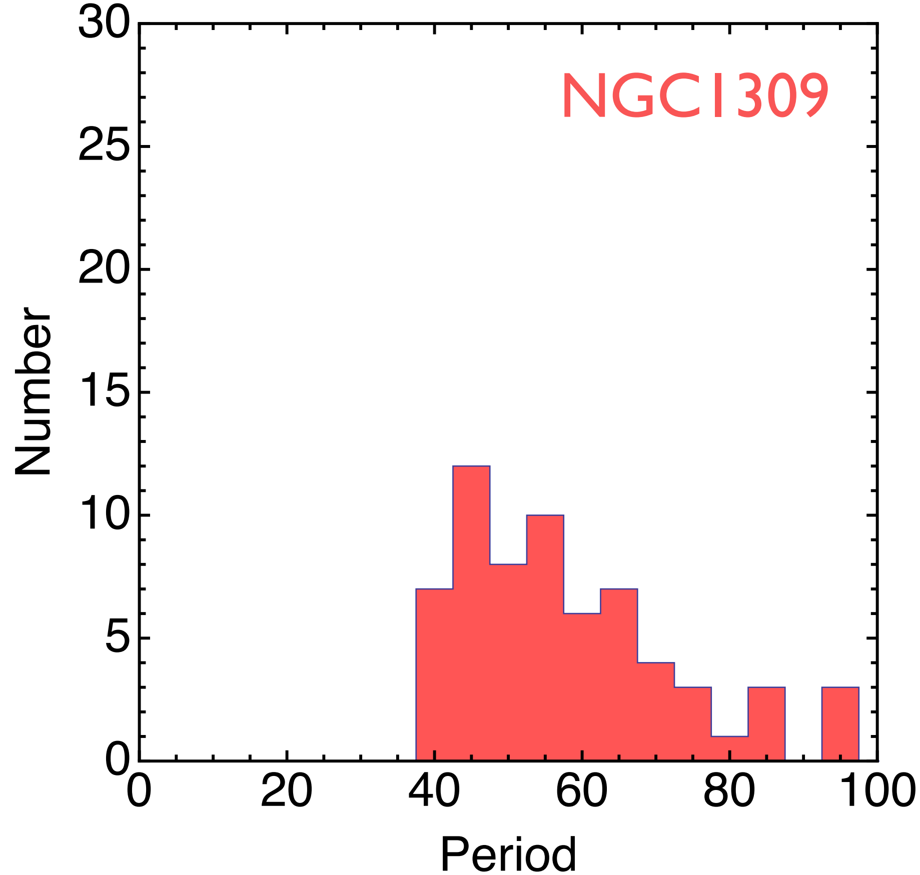

Cepheids in anchors and SNIe hosts

Do long and short period Cepheids share the same properties?

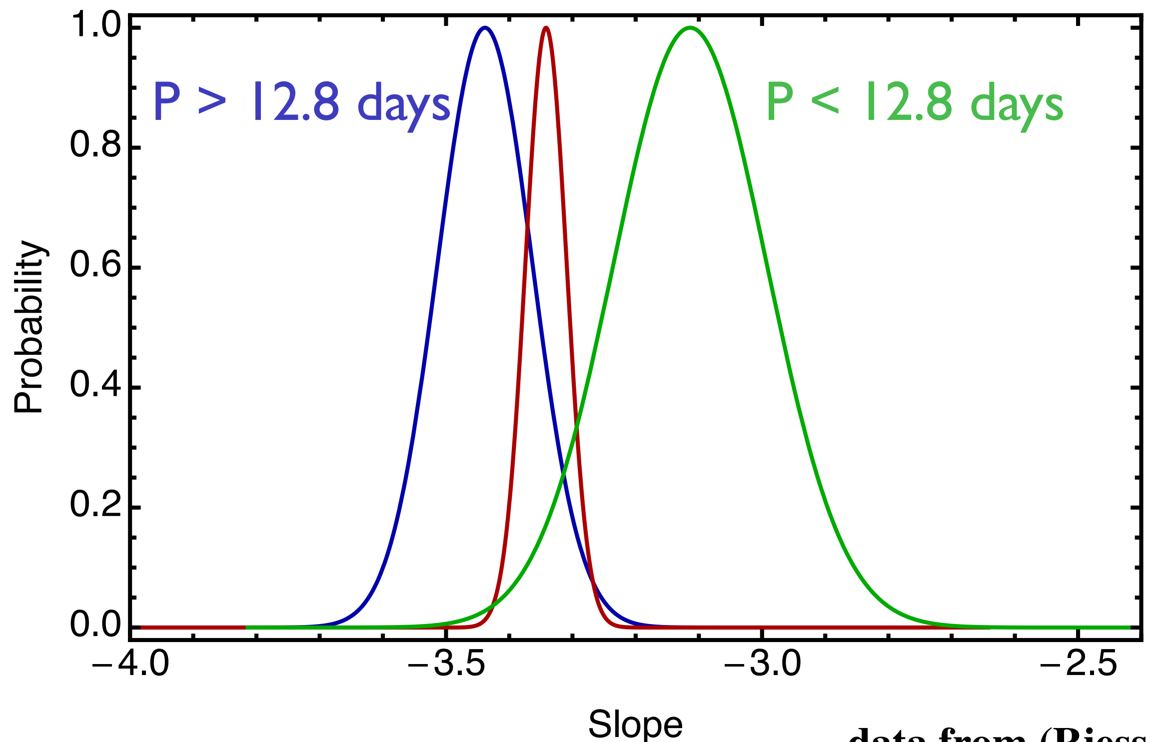

data from (Riess et al. 2019)

M101 with SN2011fe helps bridge the gap, but more long period Cepheids in anchors would increase confidence

Effect of host properties on SNe

Are the properties of the supernovae in calibrator sample the same as in the Hubble flow sample?

Brightness correlates with global properties like mass

(Sullivan et al. 2010)

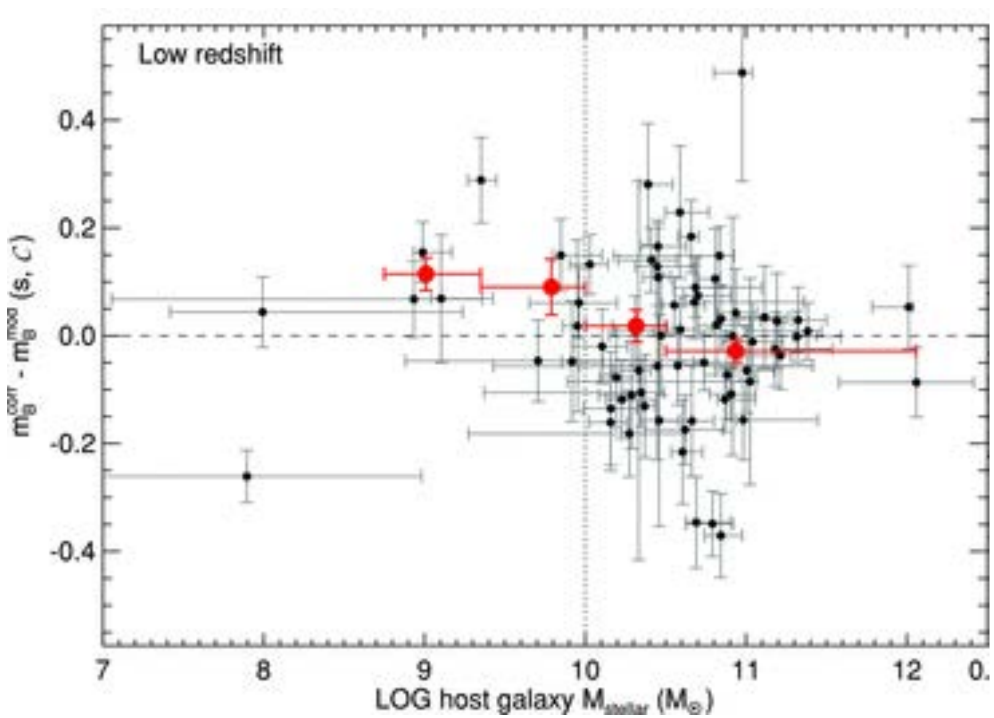

Calibrators are less massive than Hubble flow sample, and a correction is applied.

Effect of host properties on SNe

Brightness may depend on local specific star formation rate

(Rigault et al. 2018)

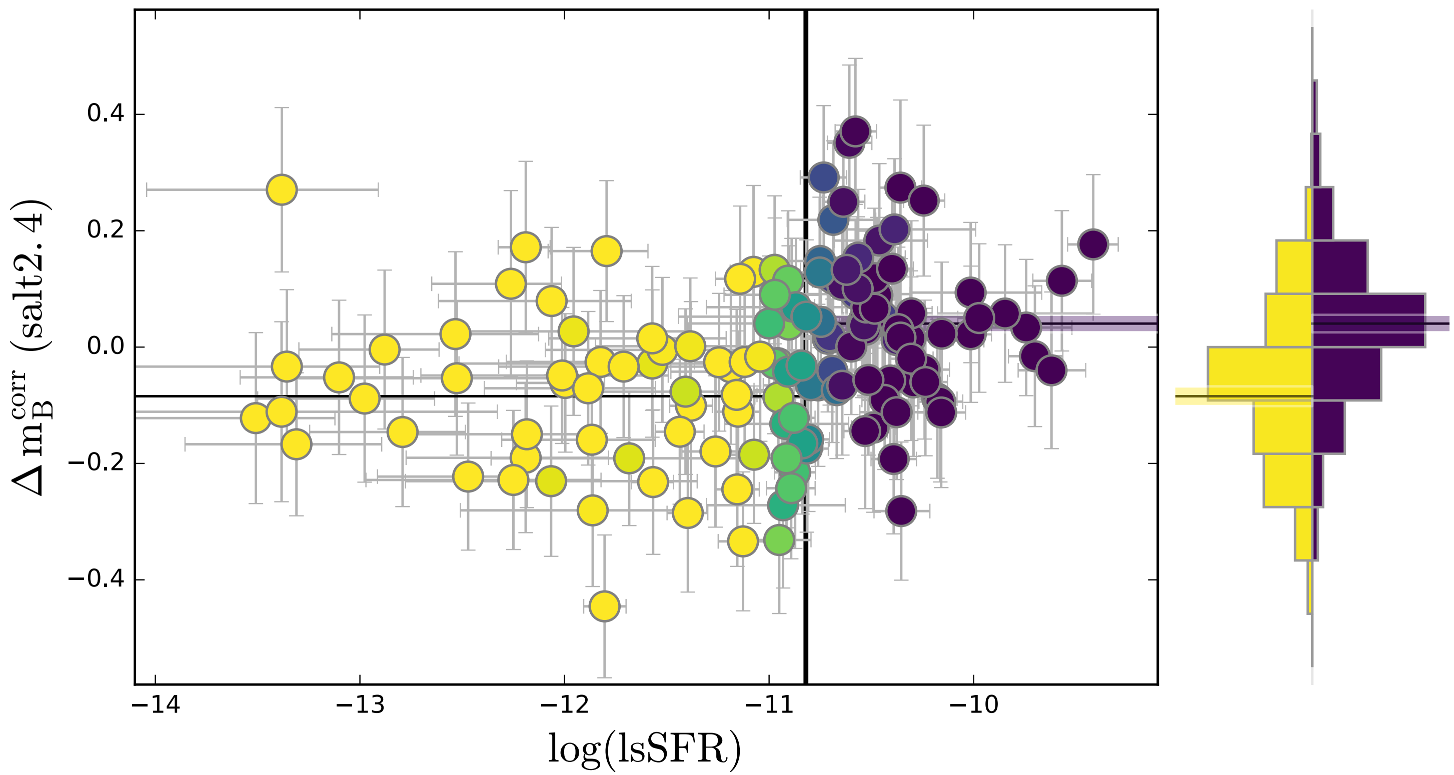

Under active debate and not yet agreed upon

Megamaser Cosmology Project

One may hope to find megamaser hosting galaxies in the Hubble flow to skip Cepheids and supernovae and directly measure H_0.

(MCP XIII)

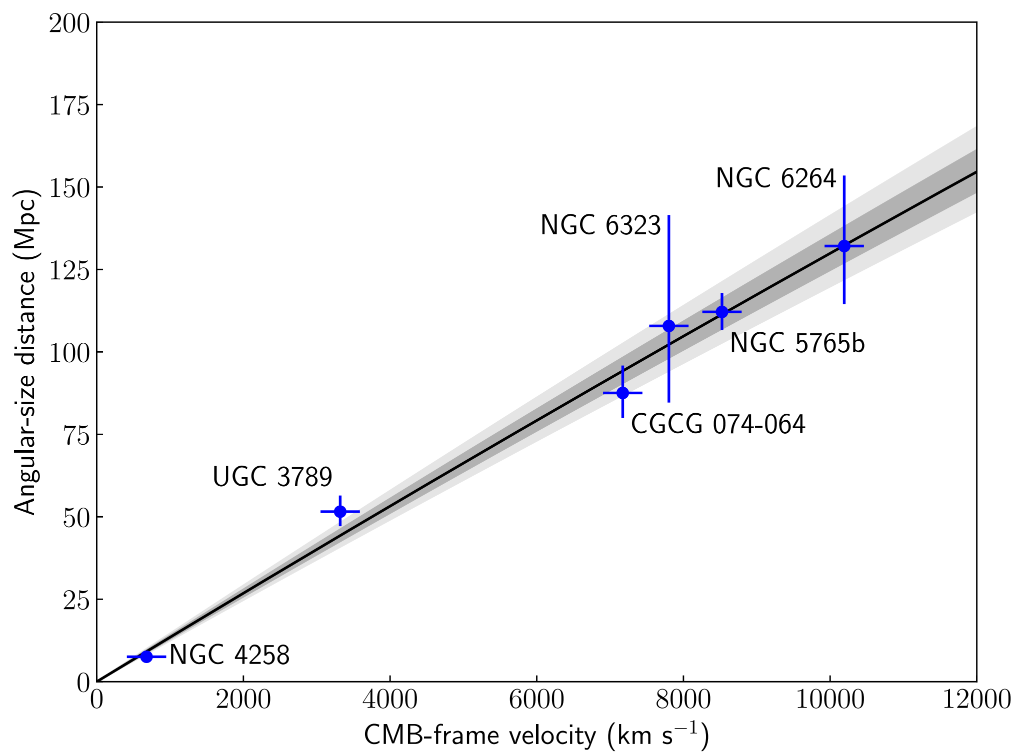

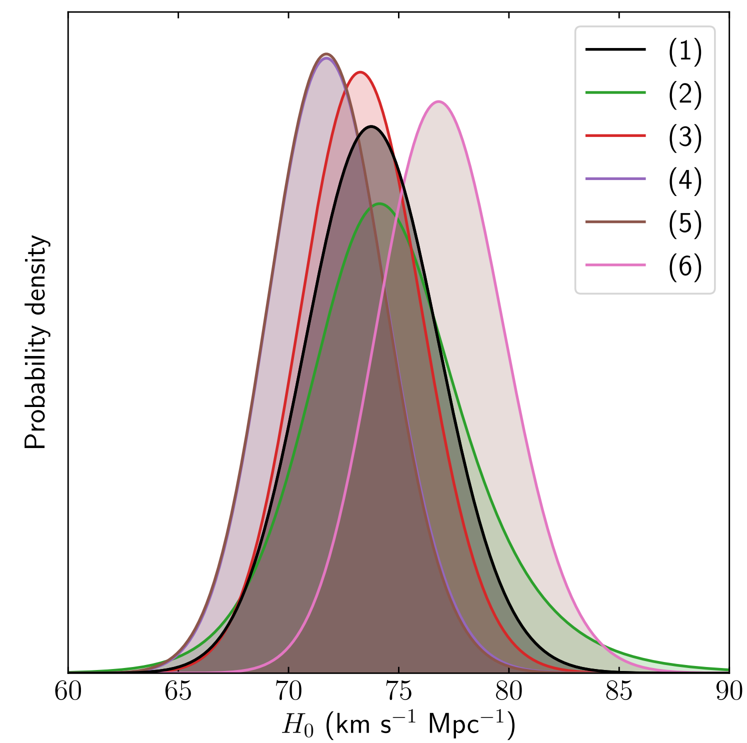

This is a reanalysis of existing data that led to several rather large shifts to higher values. Limited by number of systems.

TRGB

The tip of the red giant branch as distance indicator

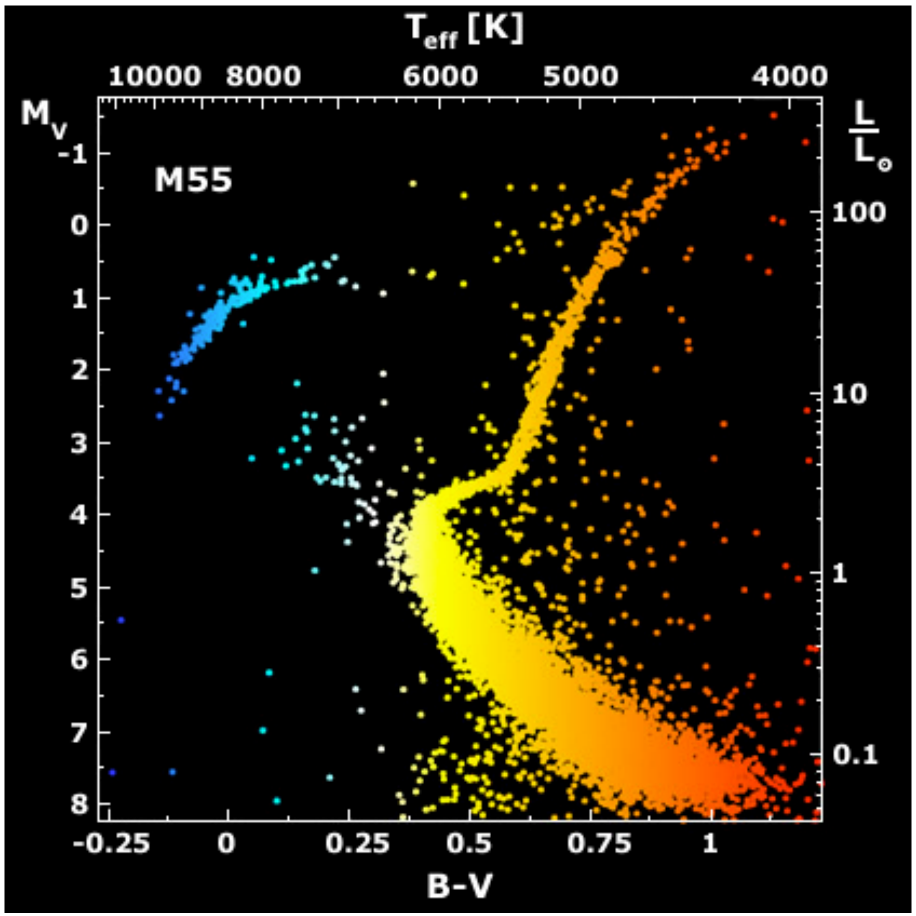

Associated with "helium flash"

Triple-alpha process becomes efficient for $T > 2 \times 10^8\, K$

reached at a core mass $M_{\rm core} \simeq 0.48 M_{\rm solar}$

thermal runaway drives stars to horizontal branch

The peak luminosity can be used as a standard candle

TRGB

The tip of the red giant branch in IC 1613

(CCHP II)

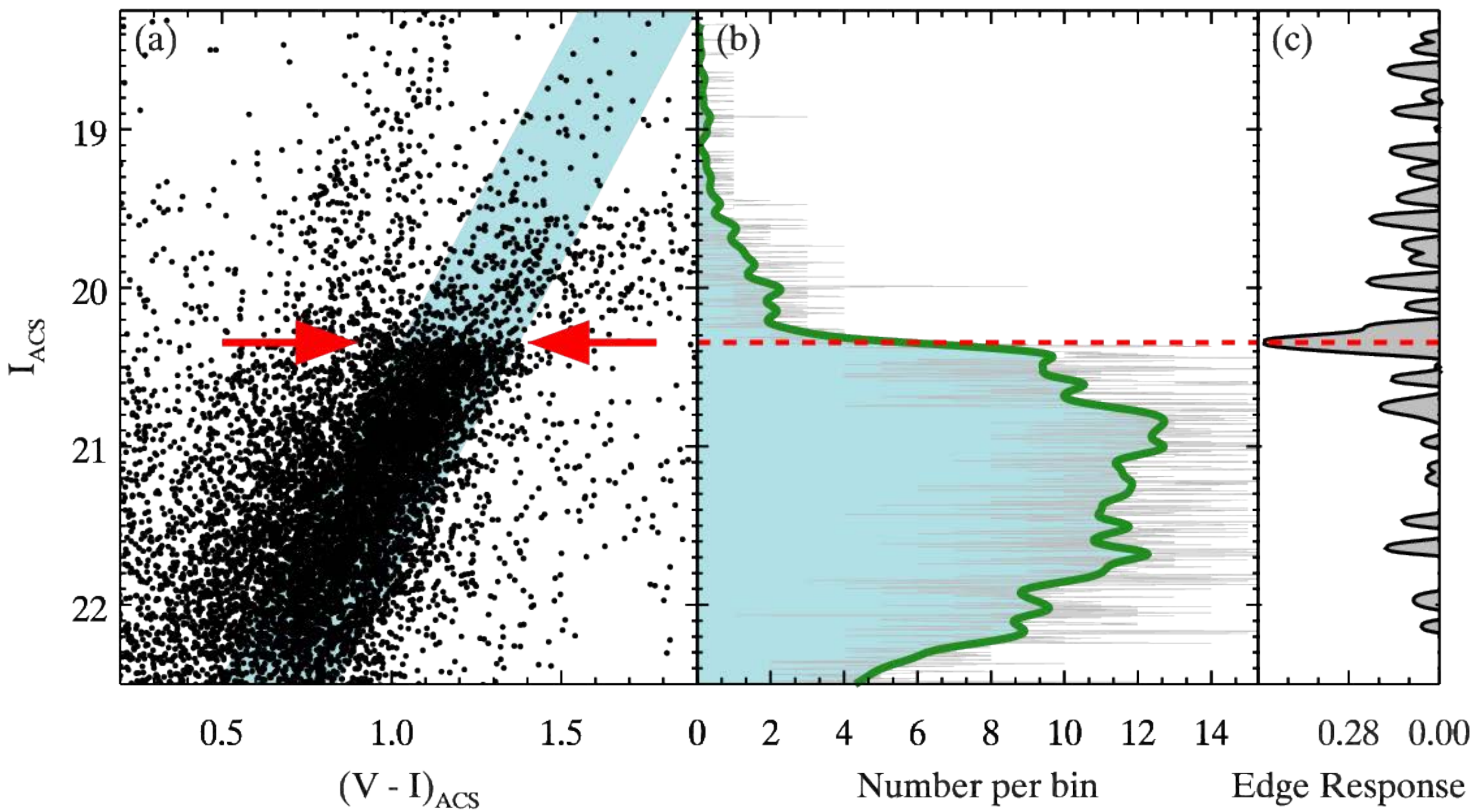

TRGB

Calibrated through systems with minimal extinction, like IC 1613 and LMC through measurement of differential distance modulus and extinction.

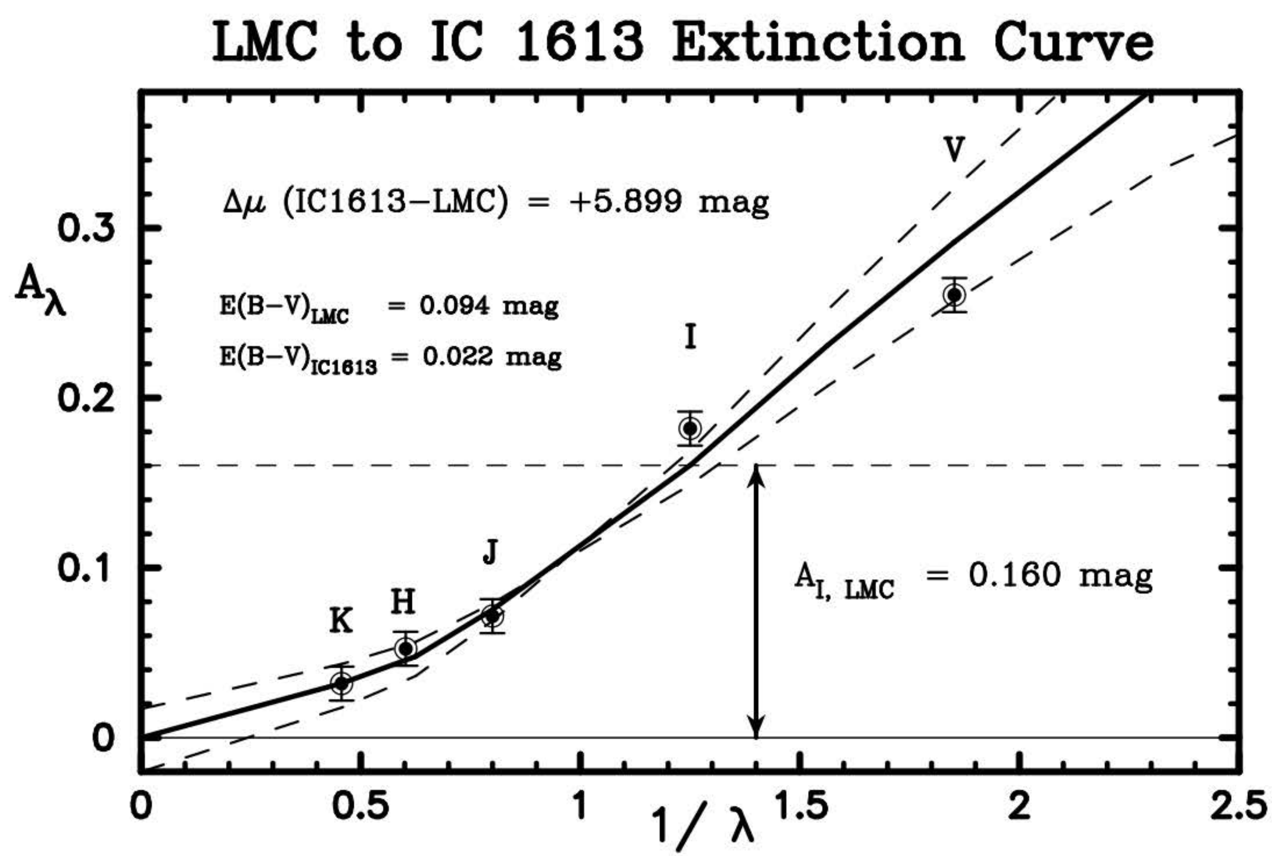

$$M_I = -4.047 \pm 0.022 \pm 0.039\,\mathrm{mag}$$

TRGB

Comparison between TRGB and Cepheid distances

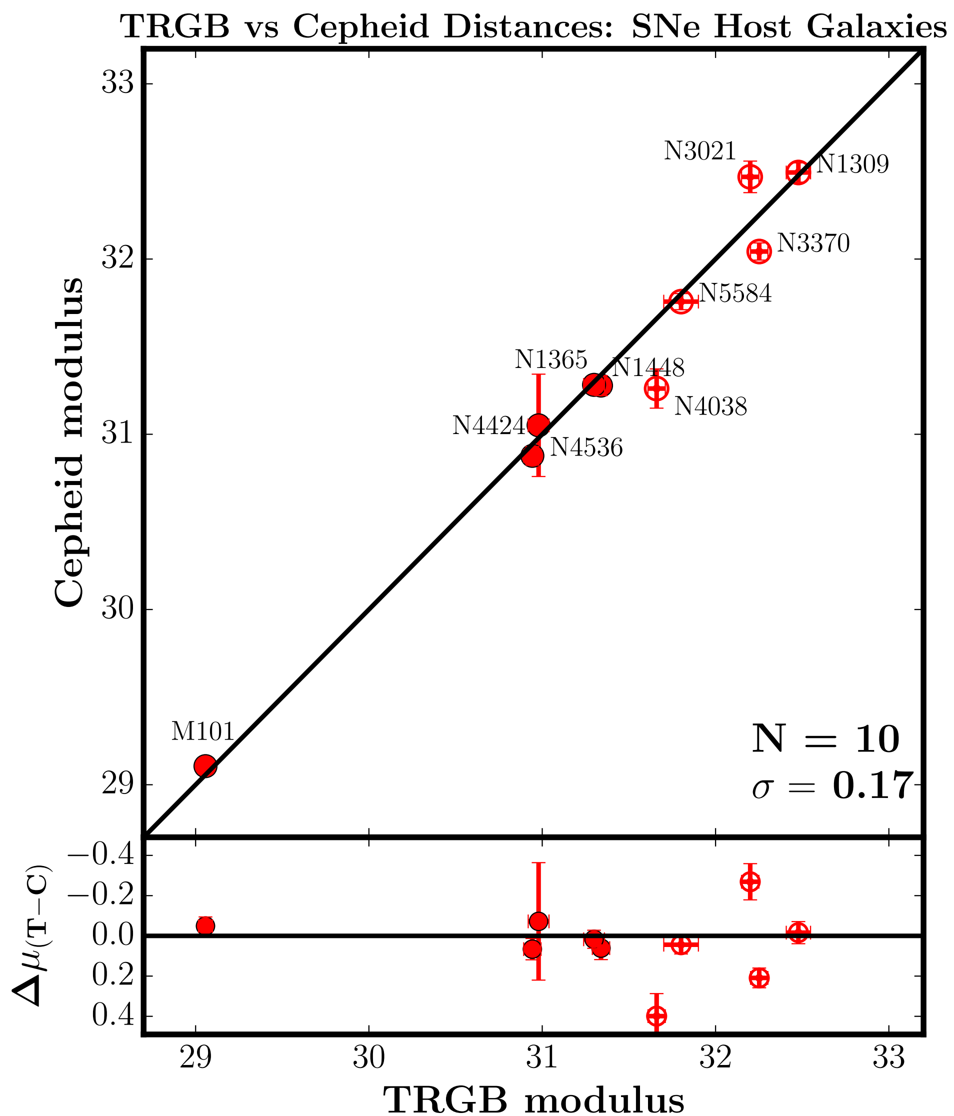

(CCHP VIII 2019)

$$\Delta\mu \simeq 0.06\,\mathrm{mag}$$

TRGB

Together with type Ia SNe, this allows to measure Hubble

(CCHP VIII 2019)

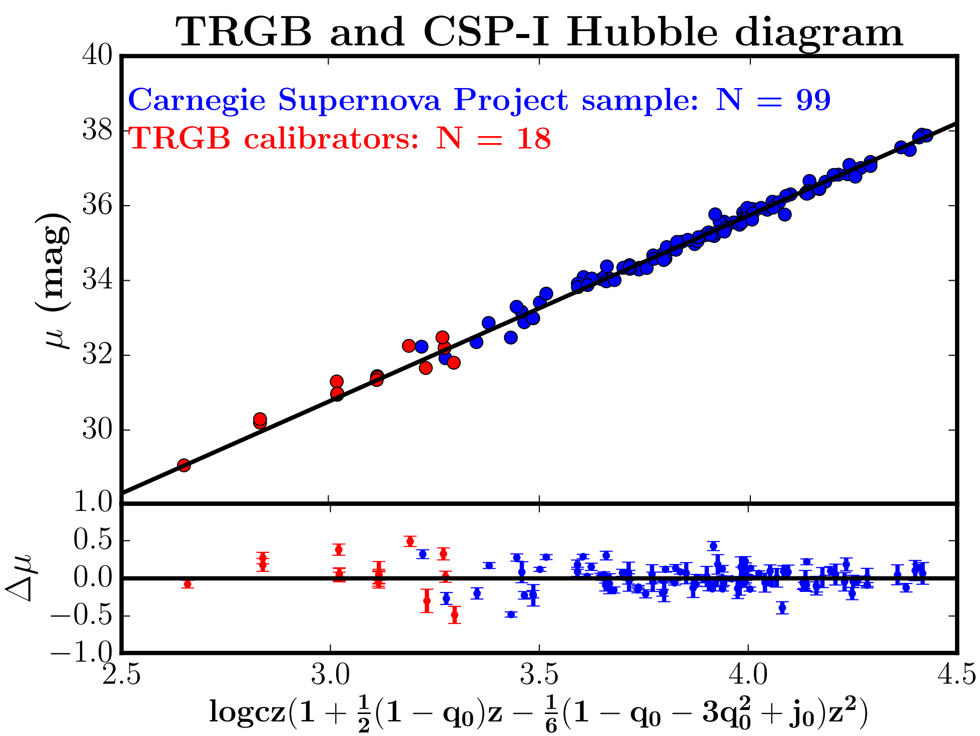

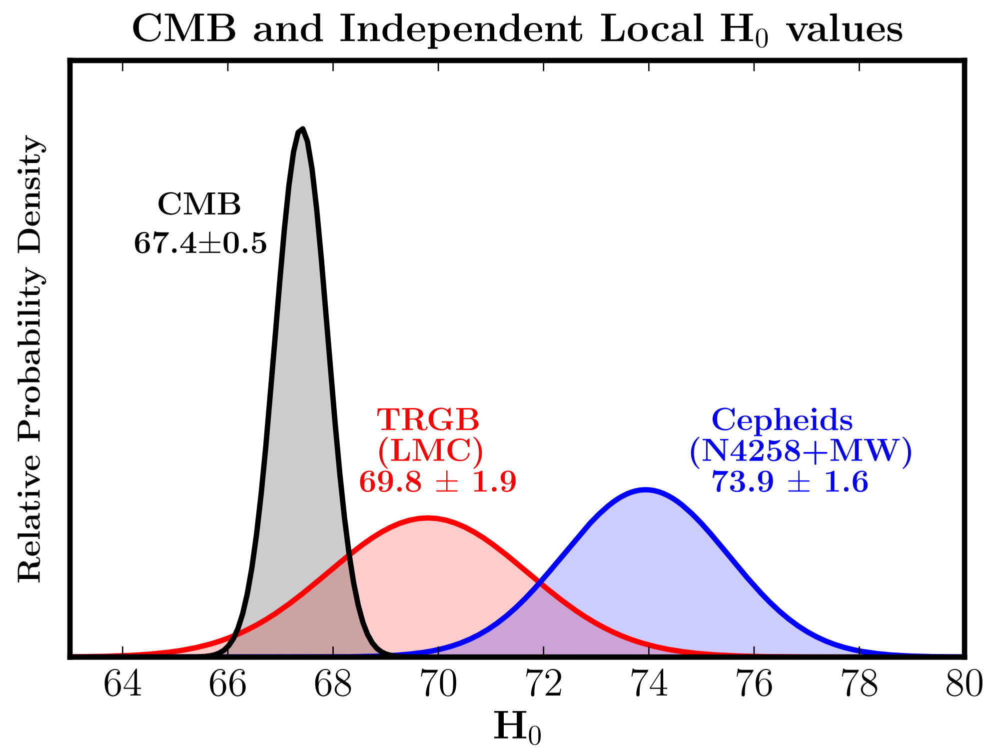

$$H_0 = 69.8 \pm 0.8 \pm 1.7\,\mathrm{km\,s^{-1}\,Mpc^{-1}}$$ **(CCHP VIII 2019)**

$$H_0 = 69.6 \pm 0.8 \pm 1.7\,\mathrm{km\,s^{-1}\,Mpc^{-1}}$$ **(Freedman et al. 2020)**

Strong lensing time delays

Lensing time delay

$$t(\theta, \beta) = D_{\Delta t} \left[\frac{1}{2}(\theta - \beta)^2 - \psi(\theta) \right]$$

with lens potential $\psi(\theta)$

and time-delay distance

$$D_{\Delta t} = (1 + z_l) \frac{D_l D_s}{D_{ls}} \propto \frac{1}{H_0}$$

Strong lensing time delays

With multiple images we may hope to measure time delay differences provided the source is time varying.

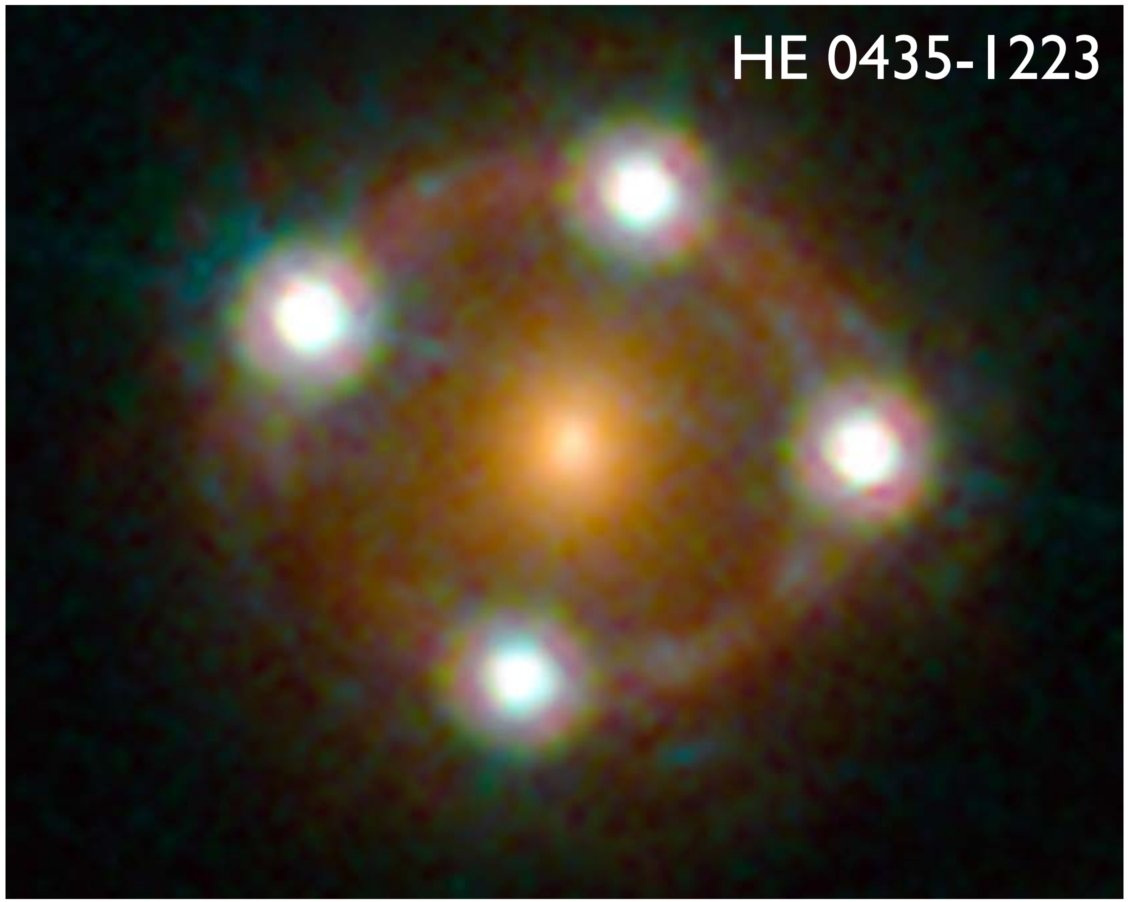

$$\Delta t_{ij} = D_{\Delta t} \left[\frac{1}{2}(\theta_i - \beta)^2 - \frac{1}{2}(\theta_j - \beta)^2 - \psi(\theta_i) + \psi(\theta_j) \right]$$

Strong lensing time delays

Together with reconstruction of lens potential $\psi(\theta)$ this allows to infer time delay distance and hence Hubble.

(H0LiCOW V)

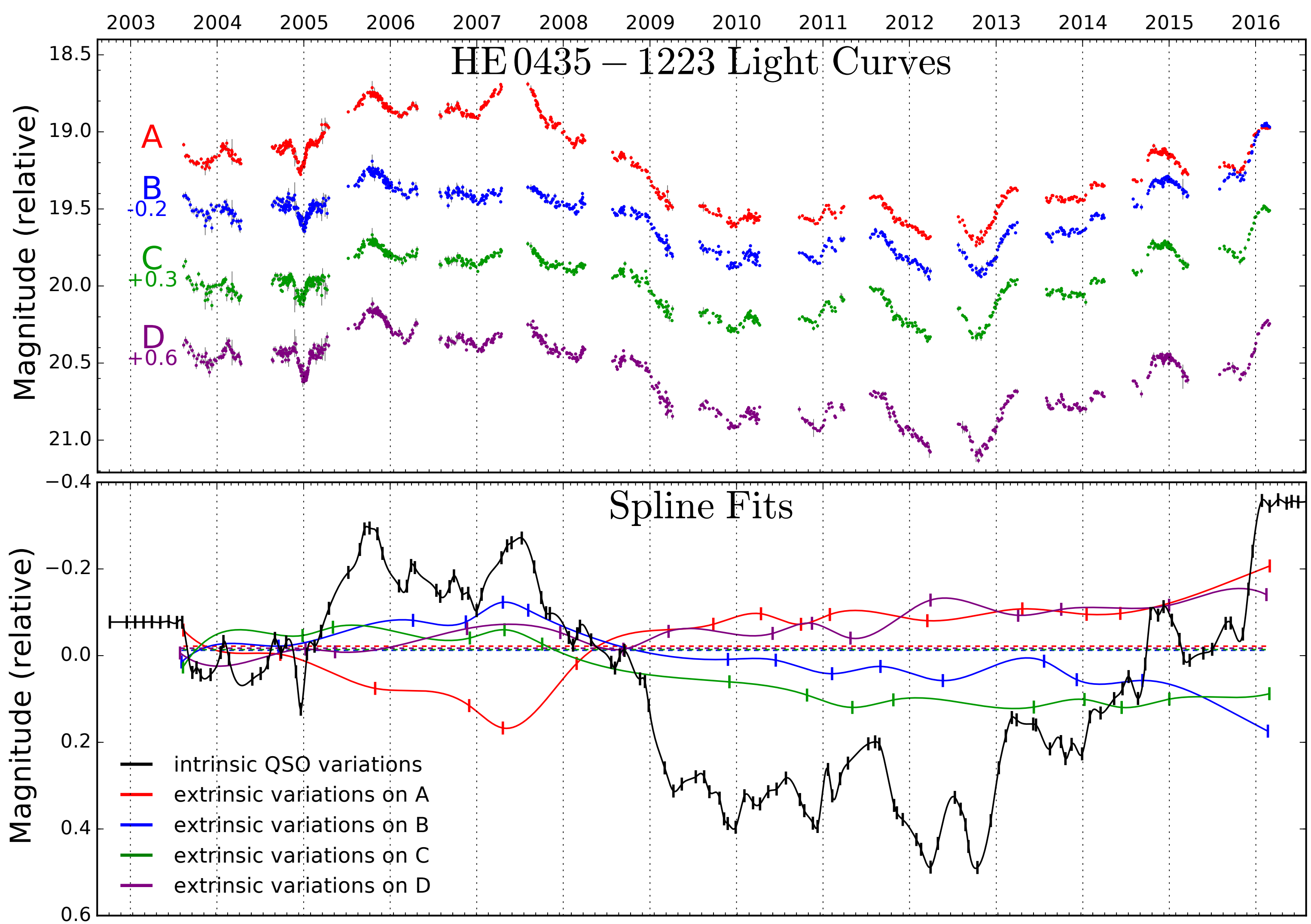

Strong lensing time delays

Lens modeling either with simple models or pixel-by-pixel

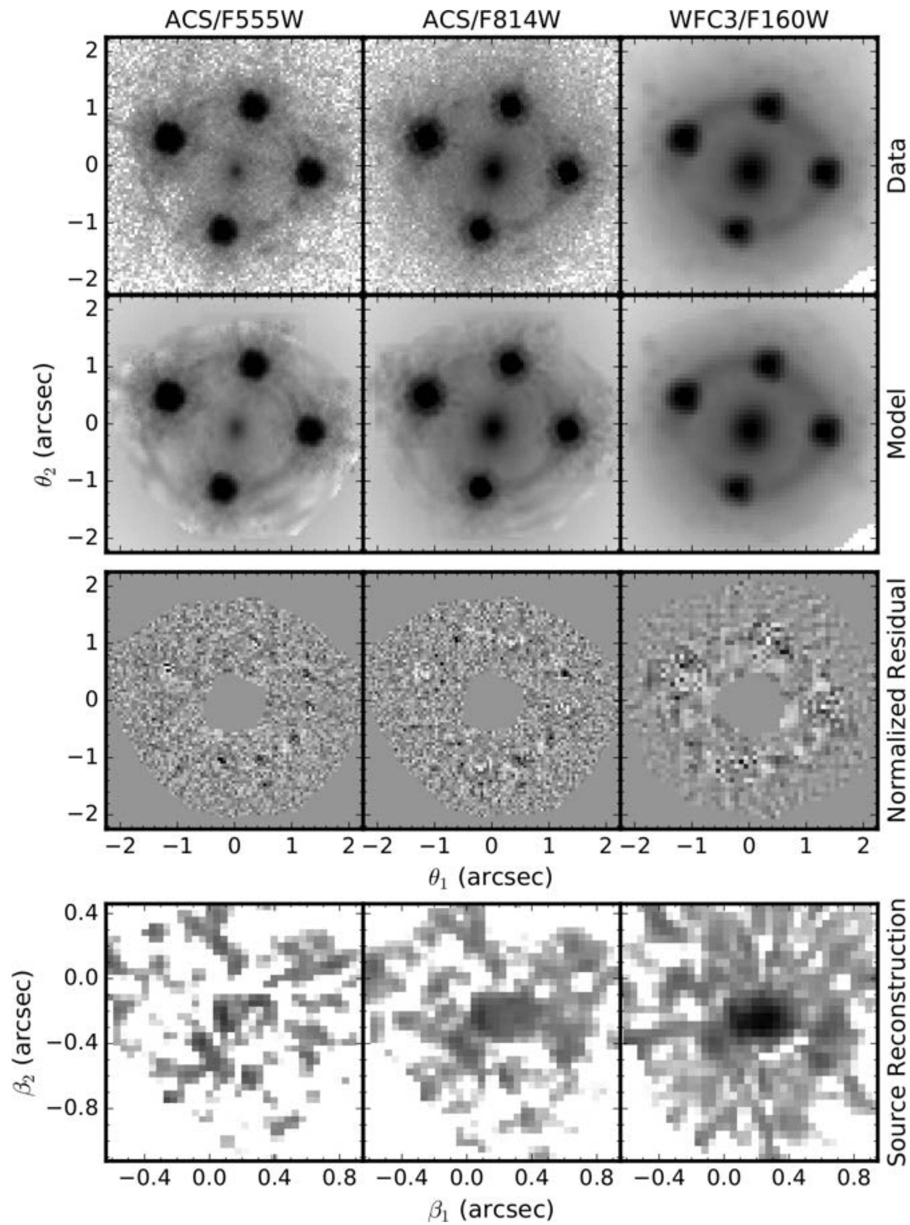

(H0LiCOW IV)

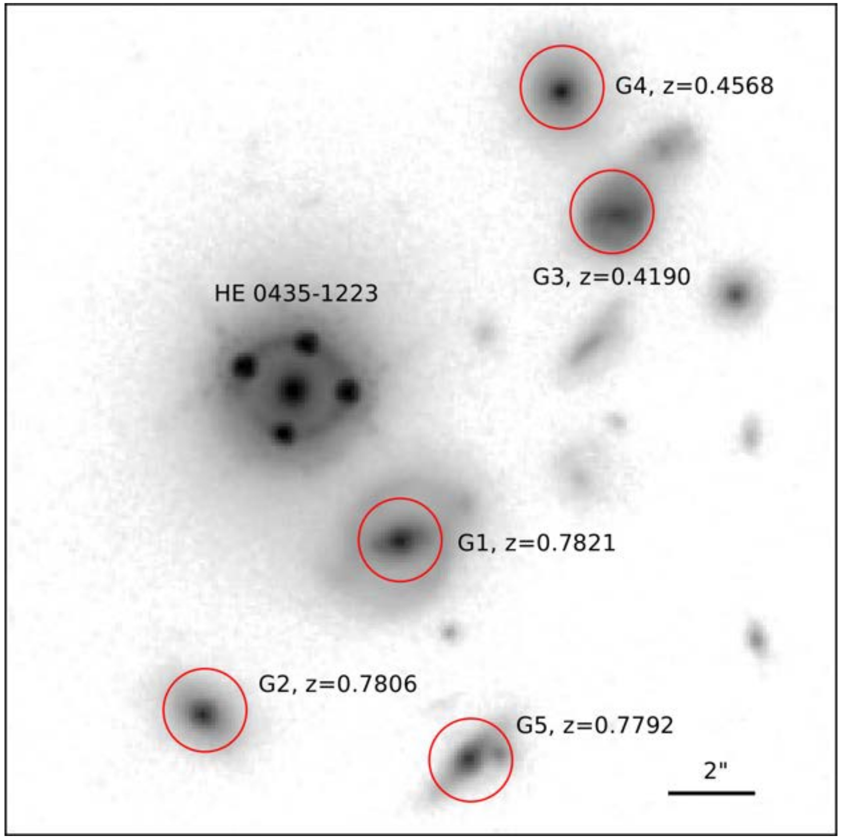

Large perturbers are included in modeling

Strong lensing time delays

Other lenses along the line of sight are included as external convergence $\kappa_{\rm ext}$, which must be inferred separately

(H0LiCOW VIII)

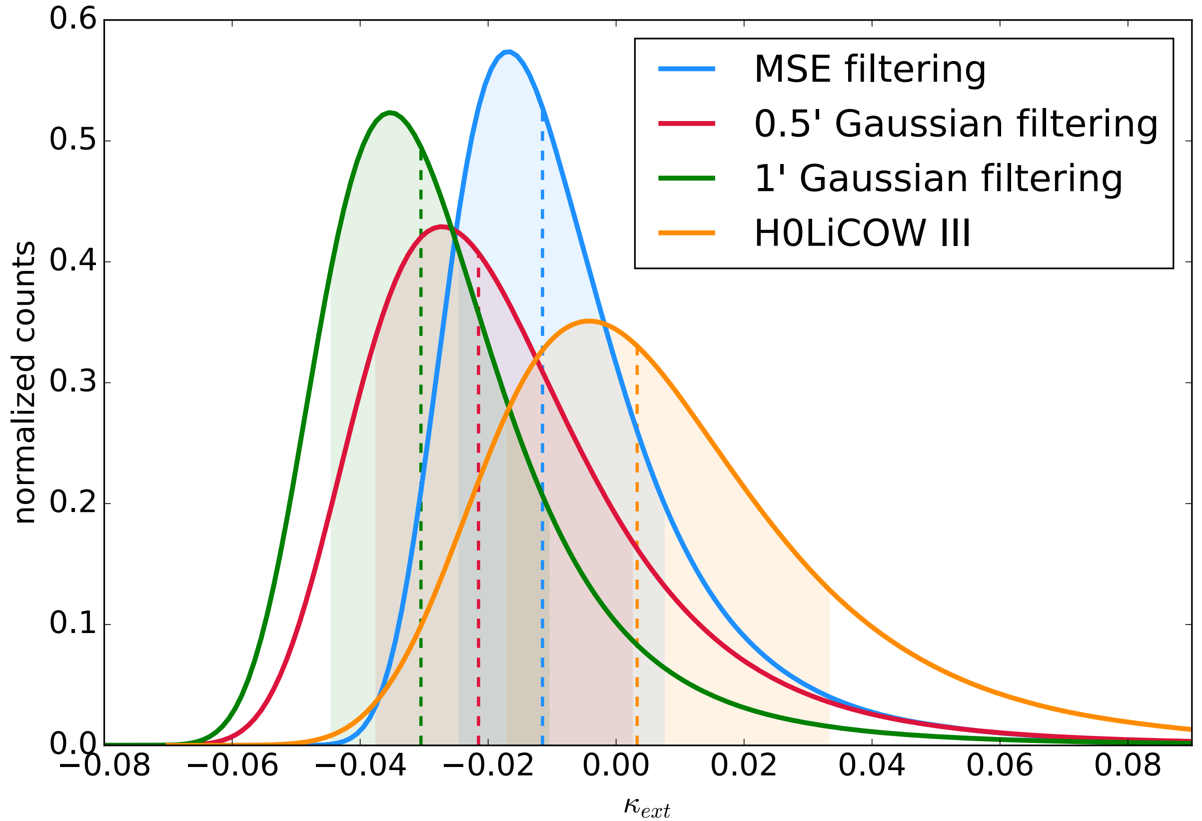

$$D_{\Delta t} = \frac{D_{\Delta t}^{\rm model}}{1 - \kappa_{\rm ext}}$$ degenerate with Hubble

Strong lensing time delays

For six strongly lensed quasars

(H0LiCOW VIII)

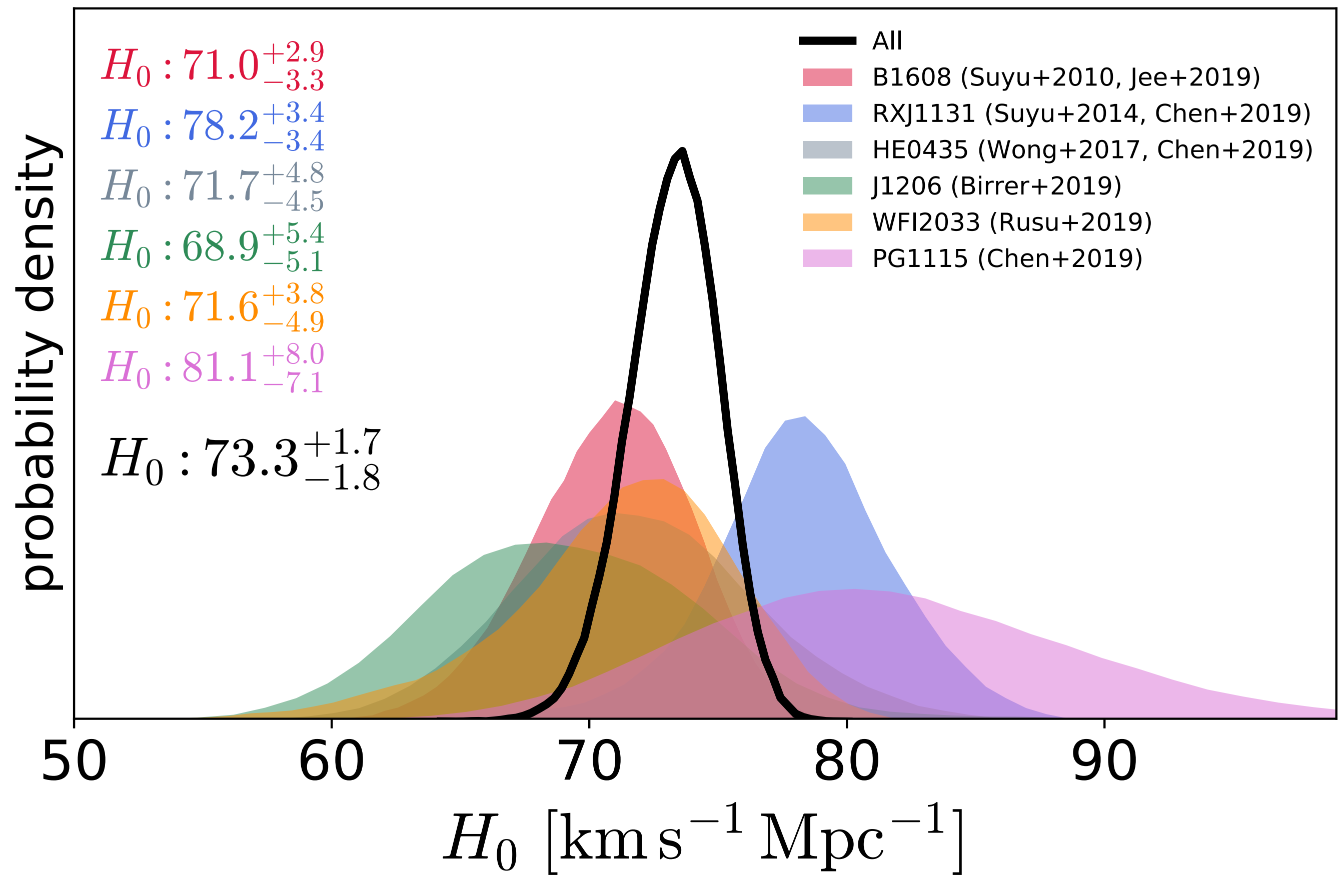

Strong lensing time delays

Data currently show a 2σ trend with lens redshift

(H0LiCOW VIII)

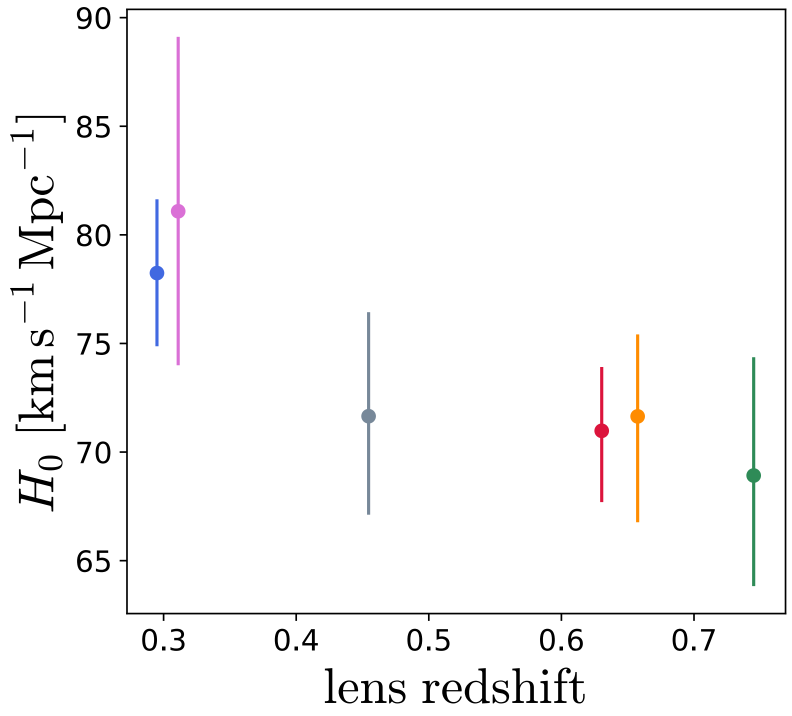

More data required to understand if this is a sign of systematics or just a statistical fluctuation.

Strong lensing time delays

Measurements of the Hubble rate from strong lensing make assumptions about the form of the density profile

(Blum et al. 2020)

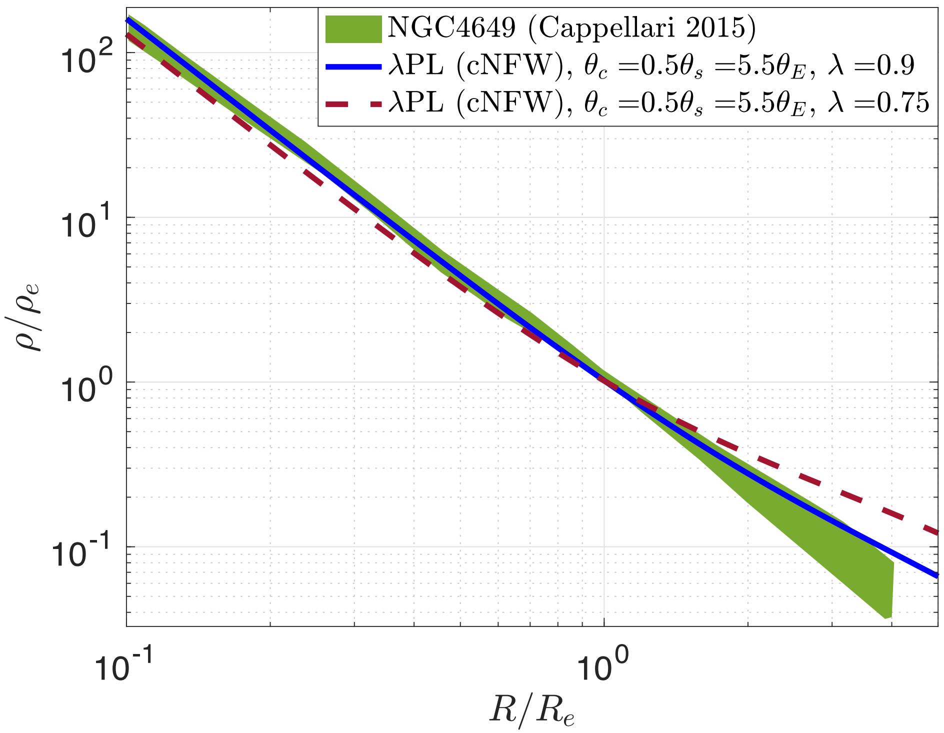

Constrained by stellar kinematics, but a core could bring measurements into agreement and does not enter the external shear

Standard Sirens

Gravitational wave observations of objects with known redshift can be used to measure Hubble

(LIGO 2017)

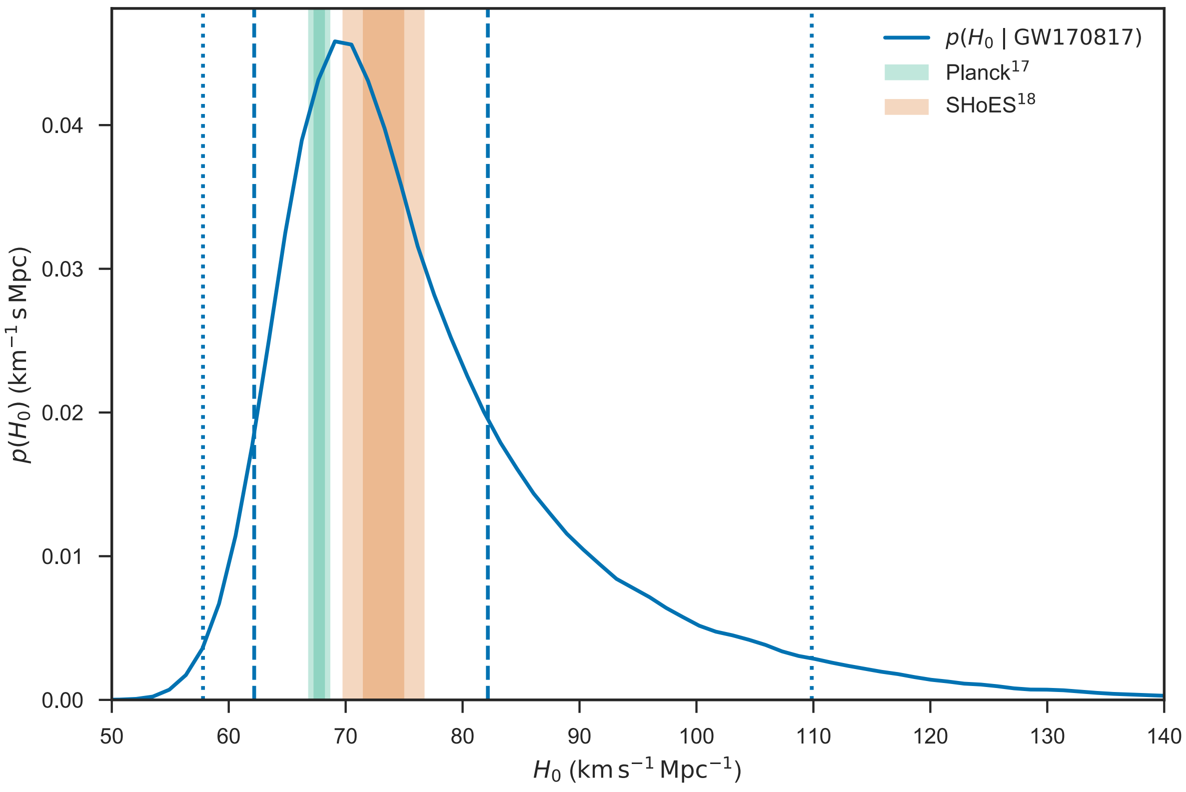

Completely independent, but require significantly more events to become competitive

Conclusions

- The precision of local measurements of the expansion rate by SH_0ES has continuously increased and measured value differs from the value predicted by Planck in the context of LCDM by 4.4σ .
- Large scale structure and supernova data make a resolution of this tension by a change to the expansion history after recombination essentially impossible, at least in context of FLRW.
- Changes to the "early" universe must occur around or just before recombination, and are tightly constrained.
- New local measurements based on the TRGB find lower values of the expansion rate and may point to systematics in Cepheid based determination.
- More data is needed (and on the way) and will resolve the issue, but in the meantime there is still room for theoretical ideas

Thank you